



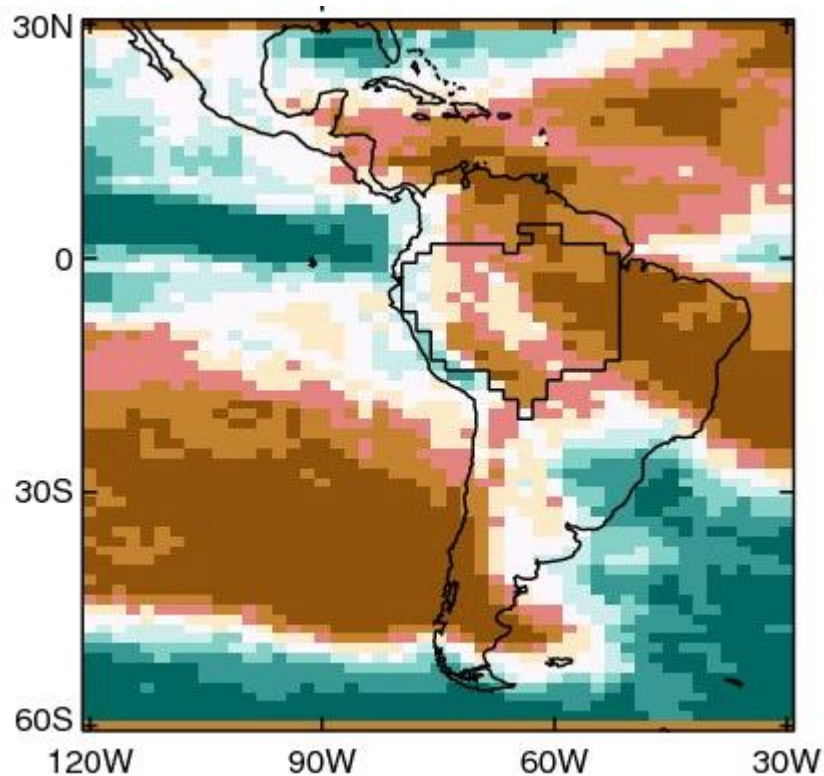
# AMAZALERT Delivery Report

Title	Report on impacts of climate change and IPCC RCP land use scenarios in Earth System Models
Work Package Number	3
Delivery number	3.1
First author	G. Kay
Co-authors	L. Alves, R. Betts, J.-P. Boisier, P. Boorman, M. Cardoso, P. Ciais, N. de Noblet-Ducoudré, H. Dolman, E. Joetzjer, C. Jones, K. Halladay, J. Marengo, C. Mathison, A. Meesters, C. Nobre, G. Sampaio, C. Seiler
Date of completion	15 February 2013
Name leading Work Package Leader	G. Kay
Approved by the Leading Work Package Leader	YES / NO

## To complete by the Coordinator

Approved by the Coordinator	YES
Date of approval by the Coordinator	18 February 2013

## Report on impacts of climate change and IPCC RCP land use scenarios in Earth System Models



**Author(s):** G. Kay, L. Alves, R. Betts, J.-P. Boisier, P. Boorman, M. Cardoso, P. Ciais, N. de Noblet-Ducoudré, H. Dolman, E. Joetzjer, C. Jones, K. Halladay, J. Marengo, C. Mathison, A. Meesters, C. Nobre, G. Sampaio, C. Seiler

**Date:** 15 February 2013

## Table of Contents

<b>Abbreviations and acronyms .....</b>	<b>4</b>
<b>Executive Summary .....</b>	<b>5</b>
Using the latest models and greenhouse gas concentration scenarios .....	5
Model representation of the climate of Amazonia .....	5
Projections of climate change .....	6
Role of land use change .....	7
Notes and recommendations .....	8
<b>1. Introduction.....</b>	<b>9</b>
CMIP3 projections of change .....	9
Climate-induced biome change.....	11
Report structure.....	13
<b>2. Description of RCP storylines.....</b>	<b>13</b>
<b>3. Description of models .....</b>	<b>16</b>
CMIP5 ensemble.....	17
HadGEM2-ES .....	17
IPSL-CM5A .....	19
<b>4. Baseline validation .....</b>	<b>20</b>
Mean state and seasonal cycle .....	20
Teleconnections with the tropical Pacific and Atlantic.....	23
<b>5. CMIP5 historical runs and projections of change in Amazonia.....</b>	<b>27</b>
Projections and seasonality .....	27
Future teleconnections with tropical Pacific and Atlantic .....	32
<b>6. Role of CMIP5 Land Use: historical and future.....</b>	<b>34</b>
Projected land-use changes in the Amazon: RCPs and other scenarios.....	35
<b>7. Summary.....</b>	<b>37</b>
<b>References.....</b>	<b>39</b>
<b>Publications .....</b>	<b>44</b>

## Abbreviations and acronyms

AR4/5	IPCC Assessment Report 4/5
CMIP3/5	Coupled Model Intercomparison Project phase 3/5
CRU	Climatic Research Unit, University of East Anglia UK
DGVM	Dynamics Global Vegetation Model
DJF	December-January-February
ENSO	El Niño-Southern Oscillation
ESM	Earth System Model
FAO	Food and Agriculture Organization
FRA	FAO Forest Resources Assessment
GCM	Global Climate Model
GHG	Greenhouse Gas
HadGEM2-ES	Met Office Hadley Centre's Global Environmental Model version 2 Earth System configuration
INPE	Instituto Nacional de Pesquisas Espaciais, Brazilian National Institute for Space Research
IPCC	Intergovernmental Panel on Climate Change
IPSL	Institut Pierre Simon Laplace, France
IPSL-CM5	Fifth generation climate model of IPSL
ITCZ	Inter-Tropical Convergence Zone
JJA	June-July-August
LAI	Leaf Area Index
LCC	Land Cover Change
LSM	Land Surface Model
LUC	Land Use Change
LUCID	Land-Use and Climate, IDentification of robust impacts project
LUH	Land Use Harmonization data set
LULCC	Land Use/Land Cover Change
MAM	March-April-May
MOSES II	Met Office Surface Exchange Scheme version 2
ORCHIDEE	Land-surface scheme of the IPSL models
PCMDI	Project for Climate Model Diagnosis and Intercomparison
PFT	Plant Functional Type
RCP	Representative Concentration Pathway
RF	Radiative Forcing
SECHIBA	IPSL land-surface scheme
SON	September-October-November
SRES	Special Report on Emissions Scenarios
SST	Sea Surface Temperature
STOMATE	IPSL carbon and vegetation model
TAG	Tropical Atlantic Gradient
TRIFFID	Met Office vegetation dynamics model
TRIP	River routing model

## Executive Summary

This Deliverable reports on the new simulations from the fifth phase of the Coupled Model Intercomparison Project (CMIP5) projections of climate change in the Amazon basin. The centennial simulations have been carried out according to different scenarios of greenhouse gas (GHG) concentrations, and include land use change consistent with development pathway and policy decisions. Thus, the implications of IPCC GHGs and land use according to the Representative Concentration Pathways (RCPs) on the changes in Amazonia can be explored in the CMIP5 multi-model ensemble. It presents an update to the last major phase (CMIP3) model projections of change that were reported in the IPCC AR4 (IPCC 2007).

### Using the latest models and greenhouse gas concentration scenarios

AMAZALERT takes advantage of the state-of-the-art in ensemble model projections of climate change available through the CMIP5. The CMIP5 modelling protocol considers a number of scenarios describing the evolution of anthropogenic drivers of climate, such as fossil fuel emissions and land use change (Moss et al. 2010), which are further used to force the climate or earth system models. The Representative Concentration Pathways (RCPs) were developed by interdisciplinary modelling frameworks to characterise a range of potential scenarios of human activities and development, and in contrast to other sets of scenarios (e.g. SRES, used to drive the CMIP3 projections of change) they account for climate mitigation policies. These RCPs describe pathways of radiative forcing and equivalent GHGs, in addition to land-use change (van Vuuren et al. 2011).

### Model representation of the climate of Amazonia

These models simulate reasonably well some aspects of the current climate of Amazonia and the wider region, such as the timing of the transitions in the seasonal cycle (Figure ES1), and the mean temperatures in the region. Many of the models capture some characteristics of the important observed relationships between rainfall and SST anomalies including being able to simulate the correct sign of the relationships between wet season rainfall and the tropical Pacific and dry season rainfall and the tropical Atlantic. However, as a whole, the ensemble simulates conditions that are too dry in the Amazon basin throughout the year, and in many models substantially so (Figure ES1).

This poses a challenge for interpreting changes in indicators of drought or other climate measures related to forest health, particularly where absolute values are thought to be important. It also has implications for the use of model output to drive offline impacts models.

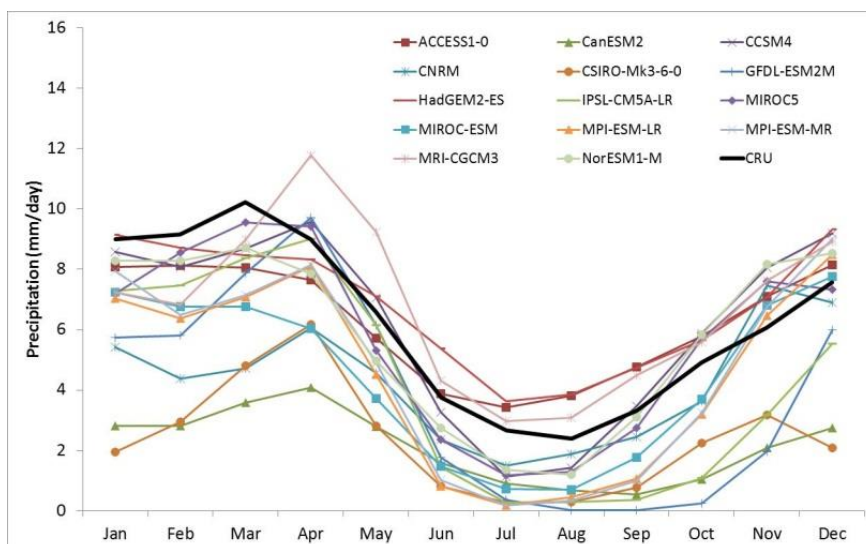


Figure ES1. Climatological seasonal cycle of and precipitation over the Amazon region in the late 20<sup>th</sup> century: CMIP5 simulations (coloured lines) and CRU observations (black line).

### Projections of climate change

The broad patterns of climate change projected by the CMIP5 ensemble are similar to those of CMIP3, and show that impacts increase under higher concentration scenarios. Temperature is projected to increase over South America (Figure ES2), with regional maximum warming occurring over Amazonia. Increasing temperature, considered in isolation from other changes, has a detrimental effect on vegetation in Amazonia (Huntingford et al. 2013 *accepted*). Therefore, temperature must always be considered a potentially important stressor on the forest.

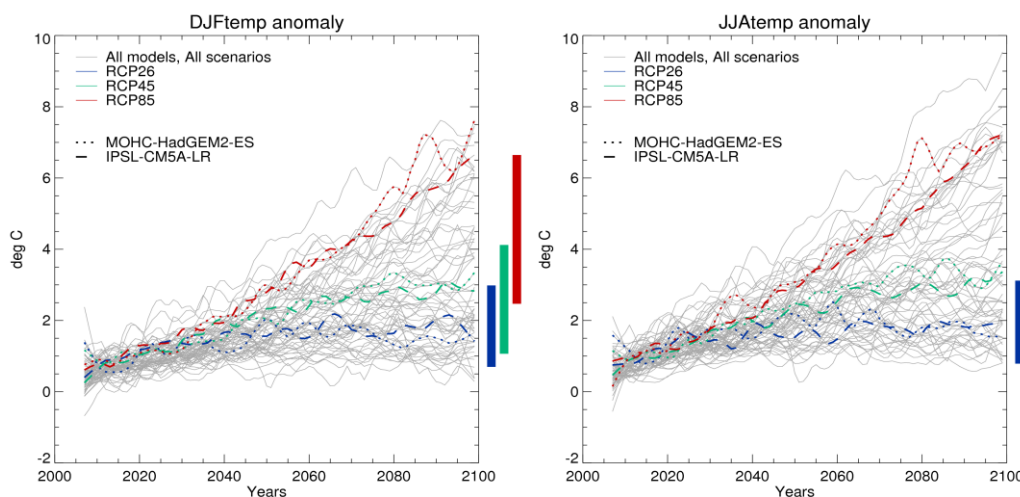


Figure ES2. Temperature change ( $^{\circ}\text{C}$ ) over the Amazon basin relative to the baseline in left: Dec-Jan-Feb (DJF); right: Jun-Jul-Aug (JJA). Grey lines show the evolution of temperature in all models for all scenarios. Projections given by HadGEM2-ES (dotted) and IPSL-CM5A-LR (dashed) are overlaid in colour: RCP2.6 (blue); RCP4.5 (green), RCP8.5 (red). Bars indicate the range in projections according to RCP for the 30-year period 2071-2100 relative to the baseline.

The availability of moisture is recognised to be of key importance for Amazon ecosystem health (e.g. Malhi et al. 2009), and a range of ecosystem services (e.g. Marengo et al. 2011a). The changes in rainfall projected by the ensemble are mixed over the Amazon basin, and vary by season. However, there is generally more agreement on drying in the eastern basin, particularly in the June to November period (Figure ES3), with wetter conditions projected by the majority of models in the western basin particularly in December to May. However, there is a spread in the model projections that spans zero, and over the Amazon basin itself, there is no clear scenario dependency apart from an increase in spread in RCP8.5 over 4.5 and 2.6.

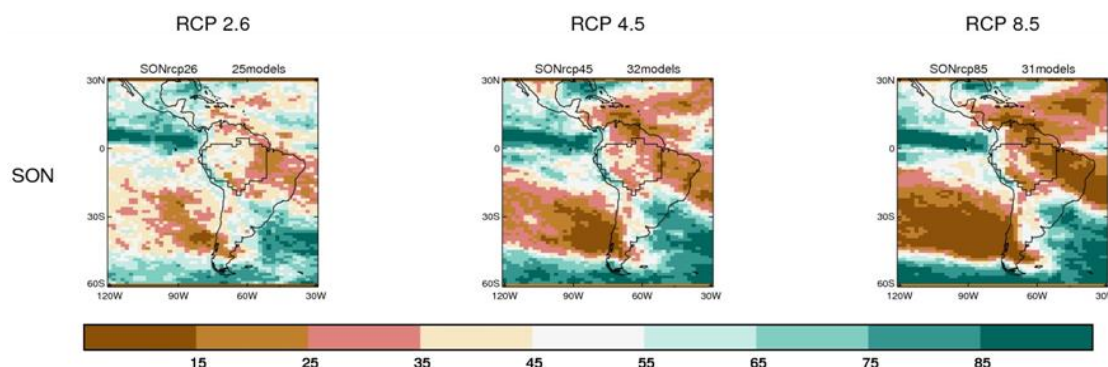


Figure ES3. Indicator of CMIP5 model consensus in precipitation changes. Percentage of models that show an increase in precipitation in Sep-Oct-Nov (SON). Number of models available for each scenario varies according to RCP and is marked above each plot. The Amazon Basin is overlaid. Brown colours indicate model agreement for a drying signal and greens for a wetting signal.

Most models projections suggest the correlation between Amazon basin precipitation and tropical Pacific SSTs in DJF will remain unchanged. In the tropical Atlantic there is little consensus on the evolution of precipitation/SST correlations in JJA, and hence it may be practical to consider only the effect of SST changes rather than changes in the precipitation/SST relationship. In most models, projections are for increased warming in the northern relative to the southern tropical Atlantic corresponding to a reduction in dry season precipitation.

### Role of land use change

Experiments complementary to the CMIP5 centennial RCP simulations were carried out in order to isolate the impacts of land use change from the other drivers of change. Land use change in Amazonia over the 21<sup>st</sup> century is small, and does not have a discernable effect on climate. A comparison between observation-based estimates of historical deforestation rates and those in the RCP with largest change (RCP2.6) reveals that the RCP rates are substantially lower. Furthermore, they are optimistic in comparison with some previously developed bottom-up scenarios (Figure ES4). It is suggested the historical land cover is not sufficiently accurate at the regional scale and also that RCP land use scenarios are unlikely to realistically represent changes at regional scales.

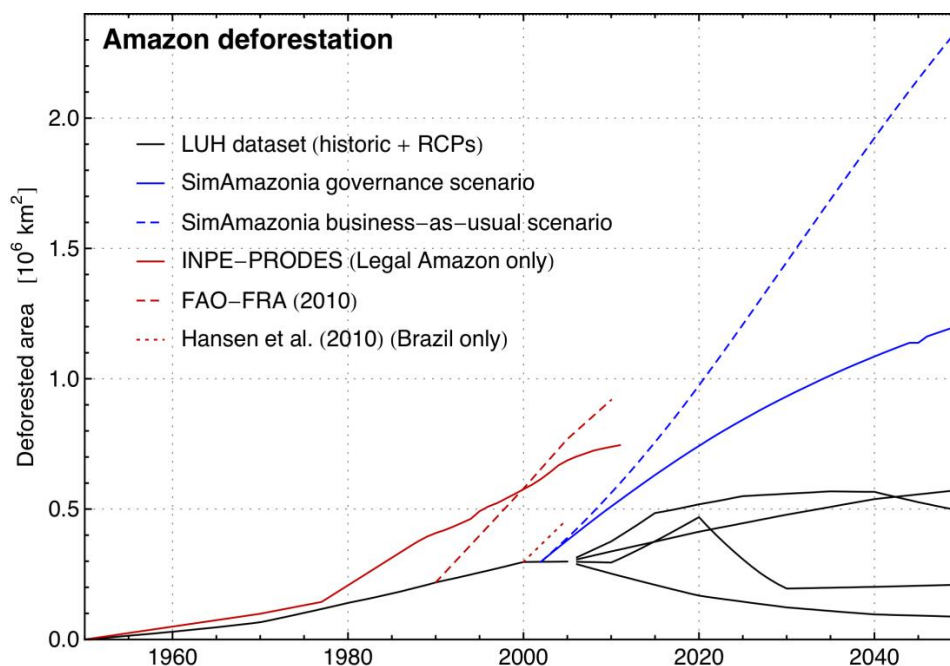


Figure ES4. Total area deforested within the Amazon basin prescribed in ORCHIDEE based on LUH data (black lines indicate the historical data and the four RCP scenarios) and based on SimAmazonia (blue; solid and dashed line indicate the governance and non-policy scenarios). Solid, dashed and dotted red lines indicate estimations of forest cover loss from different sources: PRODES (Brazilian Legal Amazon region only), FAO Global Forest Resources Assessment (2010) and Hansen et al. (2008; Brazil only). For clarity of display, the SimAmazonia and the observation-based deforestation time-series are shifted so that the first year of each matches the LUH curve.

## Notes and recommendations

The CMIP5 multi-model ensemble provides projections of climate change that sample modelling and scenario uncertainty, and which results in a range of responses in Amazonia. This allows the projections to be expressed in a way that quantifies some of the uncertainties inherent in these projections. There is strong motivation to combine the results of model runs within a multi-model ensemble, but there are many challenges associated with doing this. One way to inform the process is through validation with observations where possible. The known biases present in the CMIP5 ensemble for Amazonia should be taken into account in the interpretation of the projections of climate change, the development of Amazon ecosystem-relevant climate indicators, and in using model output to run offline impacts models.

The land use changes implemented under the RCPs are found to be insufficient for investigating impacts of land use change in Amazonia in the future, and would benefit from improved region-specific scenarios. The new scenarios of land use change being developed by INPE through AMAZALERT will help to address this requirement.

## 1. Introduction

The foremost available tools for projecting changes in climate are numerical climate models. Projections of climate change at regional scales are being increasingly used for impacts assessments and to inform adaptation planning. While a range of different options are available for model design, successive generations of ‘flagship’ models used for projections of climate change are becoming more complex. In addition, more centres are developing their own models. Model intercomparison projects have aimed to assess model similarities and differences, and have progressively set out to improve the coordination of model experiments in order to derive greater benefit from a structured modelling effort.

The primary set of models under analysis in this report come from the fifth phase of the Coupled Model Intercomparison Project (CMIP5), and experiments carried out under its coordination will form the foundation of the upcoming Fifth Assessment Report (AR5) of the Intergovernmental Panel on Climate Change (IPCC). The new emissions pathways are consistent with different scenarios of land use change, and so the impacts of climate and land use change in Amazonia can be explored within the CMIP5 projections. The last IPCC report (AR4) was published in 2007, and brought together projections from more than twenty climate models through the previous major phase of the Coupled Model Intercomparison Project (CMIP3). We begin by setting out some of the major findings from AR4 and CMIP3 for Amazonia in order to provide the context for the analysis carried out here.

### CMIP3 projections of change

The models were run according to scenarios of greenhouse gas concentrations in the atmosphere – from high emissions to low (IPCC Special Report on Emissions Scenarios, SRES: Nakićenović et al. 2000). While the same greenhouse gas forcing is applied to all models, they each give a different climate response, particularly at sub-global scales.

Analysis of the CMIP3 ensemble shows that temperatures are projected to increase substantially over the continent of South America (Figure 1, top row) while there is more of a mixed response in precipitation (middle row). Over the Amazon basin, the ensemble mean indicates a wetting signal during the wet season (Dec-Jan-Feb, DJF) and a drying signal in the dry season (Jun-Jul-Aug, JJA), particularly in the eastern basin, and with projections for wetter conditions in the western basin. However, there is a large degree of uncertainty in these projections as evidenced by the poor levels of agreement between the individual models in the sign of the change: towards wetter or drier conditions (bottom row).

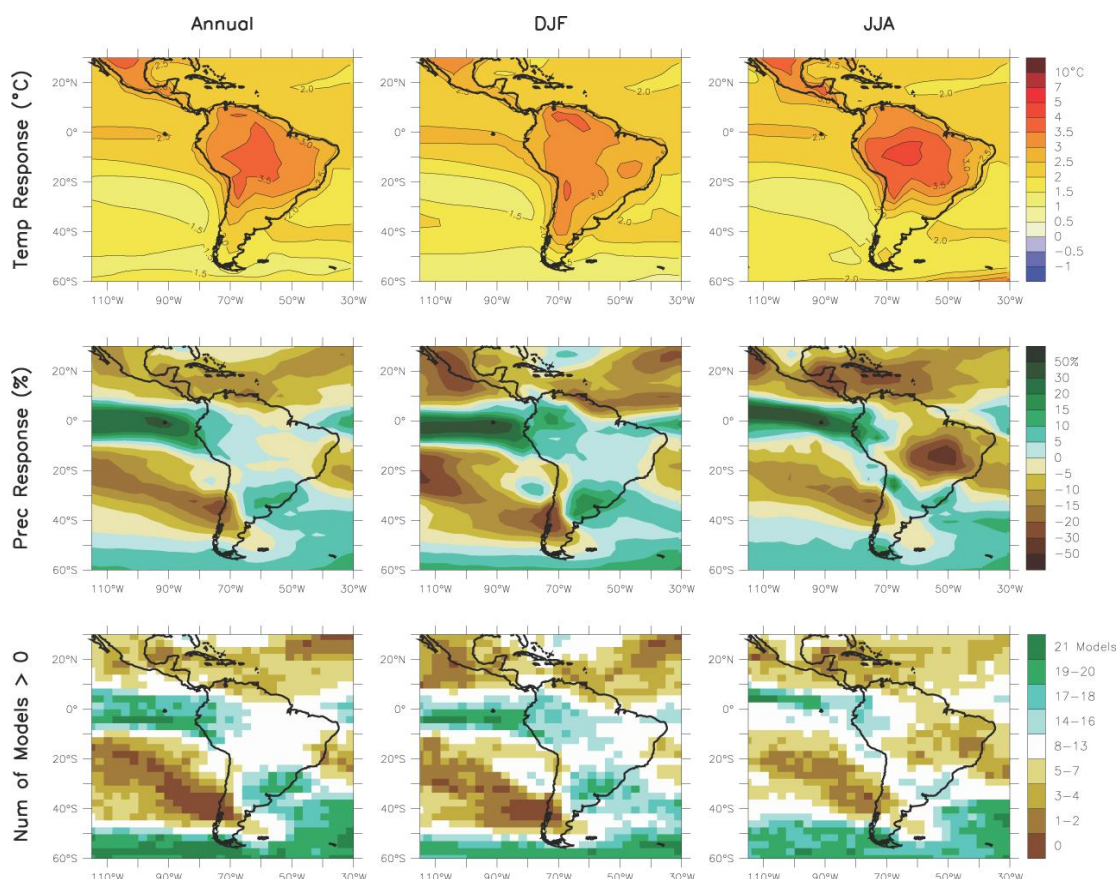


Figure 1. Temperature and precipitation changes over Central and South America from the multi-model SRES A1B simulations. Top row: Annual mean, DJF and JJA temperature change between 1980 to 1999 and 2080 to 2099, averaged over 21 models. Middle row: same as top, but for fractional change in precipitation. Bottom row: number of models out of 21 that project increases in precipitation. Source: IPCC AR4 WG1, their Figure 11.15.

The ensemble average projections shown in Figure 1 are for a single SRES scenario (A1B), but other work has shown the effect of scenario on projections of change in Amazonia in the CMIP3 models (Figure 2). The scenarios in this figure are SRES A2 (a high emissions scenario) and SRES B1 (a low emissions scenario). The projections of temperature over Amazonia show that there is a range described by the individual models in the magnitude of warming. However, all of the models project increasing temperatures, and they clearly demonstrate that following a higher emissions scenario produces larger impacts. As described above, projections of rainfall across the globe are more mixed between the models than for temperature, and this is the case for the Amazon region. The multi-model averages show very small changes, not because the models are all projecting small changes, but because some are for wetter conditions in the future and others for drier. This is true regardless of the emissions scenario. Unlike for temperature, the rainfall projections appear to be independent of emissions scenario for this multi-model ensemble.

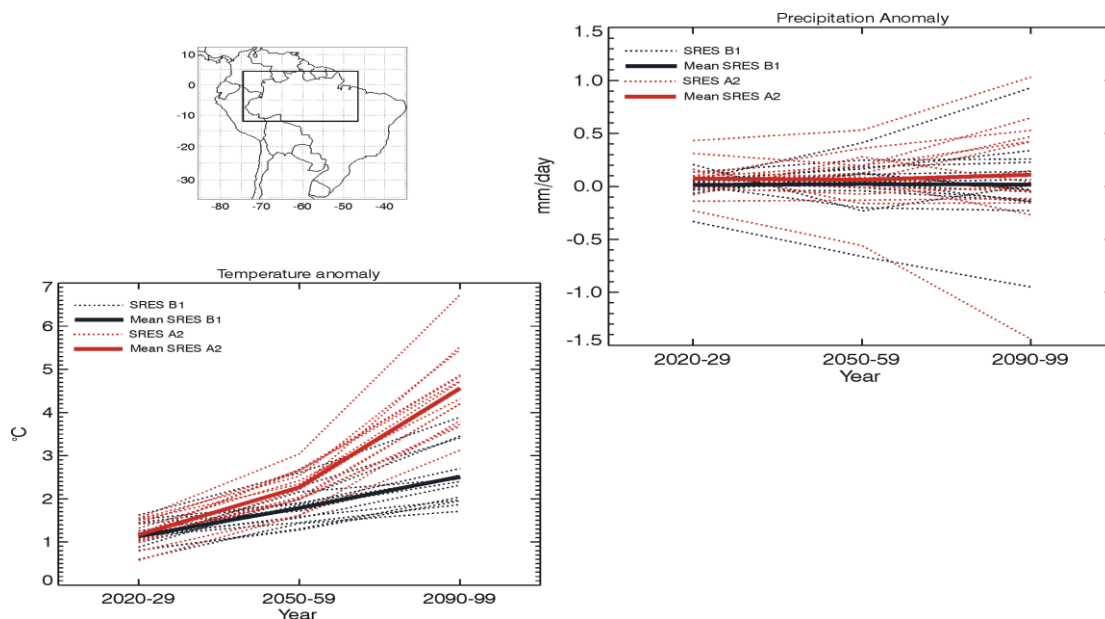


Figure 2. Changes in temperature (bottom left) and rainfall (top right) for the periods 2020-2029, 2050-2059 and 2090-99 with respect to the 1961-1990 average, simulated by 15 different climate models submitted to the IPCC AR4 for a high (red; SRES A2) and a low (black; SRES B1) scenario. The projected changes are averaged over Amazonia (box in map). The bold lines show the average of the 15 models included in this study for each scenario, and the dotted lines show individual model projections. Source: Marengo et al. (2011a), their Figure 7.

### Climate-induced biome change

The Met Office Hadley Centre HadCM3 family of global models are known to simulate strong warming and drying of the climate in Amazonia during the 21st century. Besides the direct implications of higher temperatures and lower rainfall, some of the first experiments using coupled climate-carbon cycle models indicated that there may be implications for the continued viability of the Amazon rainforest, and in turn upon the regional and global climate. In the HadCM3LC model, which includes the carbon cycle and dynamic vegetation, the climate effects on the forest led to feedbacks on the global carbon budget that amplified climate change. In this model, these large simulated climate changes and carbon cycle feedbacks produced a “die-back” of the tropical forest of Amazonia (Betts et al. 2004; Cox et al. 2000). Further studies have explored the notion of committed changes (Jones et al. 2009), whereby the vegetation lags the climate and takes longer to come into equilibrium. Therefore, even if there is little vegetation response to the climate changes projected over the 21<sup>st</sup> century, there may already be a commitment to larger changes in the biosphere in the future even if the climate does not change further.

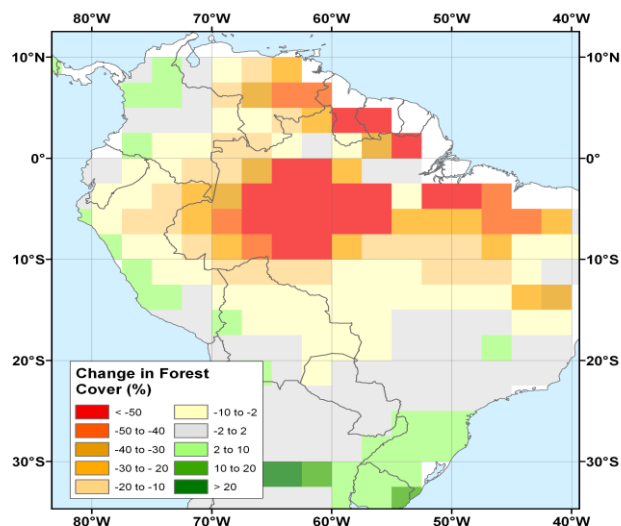


Figure 3. Percentage change in forest cover by late 21st century compared with pre-industrial conditions, as modelled using Hadley Centre coupled climate-carbon model HadCM3LC with a 'business as usual' greenhouse gas concentration scenario. Red colours indicate a reduction in forest cover. It demonstrates the 'dieback' of the forest resulting from simulated warmer and drier climate in the future, and carbon cycle feedbacks. After Cox et al. (2000).

In Amazonia, some climate and vegetation models project a shift in biome from tropical forest to seasonal forest or savanna by the end of the 21<sup>st</sup> century driven by regional climate change – increases in temperature and decreases in rainfall – in the absence of direct deforestation (Cox et al. 2000; Betts et al. 2004; Scholze et al. 2006; Malhi et al. 2009; Salazar et al. 2007; Salazar and Nobre 2010).

Malhi et al. (2009) found that the CMIP3 climate changes in the region tend to push the region towards a seasonal forest-type regime rather than savanna. Their results suggest a high probability of an intensification of the seasonality of the rainfall in Amazonia, leading to increased dry season water stress, and a medium probability that this new state will favour seasonal forest over tropical forest. They suggest that some of the negative effects of the climate change on the forest may be mitigated by ecosystem response to rising CO<sub>2</sub> and changing climate, although there are large uncertainties associated with this. Rammig et al. (2010) found from 24 general circulation models projections that the uncertainty associated with the long-term effect of CO<sub>2</sub> is much larger than that associated with precipitation change and concluded that CO<sub>2</sub> effects are one of the key unknowns in assessing the risk of Amazonian forest dieback in response to 21<sup>st</sup>-century climate change. Some more recent studies (Cox et al. 2013; Huntingford et al. 2013 *accepted*) have suggested that the Amazon forest could be more resilient to CO<sub>2</sub>-driven climate change than some of the earlier work suggested.

However, many of these studies emphasise that climate change is only one potential source of stress on the forest, and land use change in the Amazon may interact with climate changes to produce larger effects namely on the regional climate and hydrology. There is some observational evidence to that effect (Costa et al. 2003; Butt et al. 2011) and many modelling studies have demonstrated these potential effects through a range of experiments (Nobre et al., 1991; Costa and Foley 2000; Cox et al. 2000; Costa et al. 2007; Sampaio et al. 2007; Malhado et al. 2010). Overall, a common argument is that large-scale deforestation alters surface albedo, and evapotranspiration (associated with a decrease in leaf area index, a decrease in root depth, and reduction of roughness), ultimately reducing precipitation totals in the Amazon (Nobre et al., 1991; Costa and Foley 2000; Costa et al. 2007; Sampaio et al. 2007), and may increase the duration of the dry season (Costa and Pires 2010). This could translate in changes in fire frequency (Nepstad et al., 1999) and nutrient cycle feedbacks (Senna et al. 2009), which could lead to changes in vegetation composition and structure (Cox et al. 2000; Malhi et al. 2009; Rammig et al. 2010; Salazar and Nobre 2010), affect water resources (Coe et al. 2009) and carbon emissions (Cox et al. 2004).

## Report structure

In this Deliverable, we take advantage of the new phase of the Coupled Model Intercomparison Project, CMIP5, and the newly developed emissions storylines that underlie the Representative Concentration Pathways (RCPs). We begin by describing the RCP storylines, in terms of radiative forcing and the impact of different development pathways on land use change. Next, we describe the models used in projections for Amazonia. We provide an overview of CMIP5 ensemble and then describe in greater detail the models from the AMAZALERT partners Met Office and IPSL, because over the course of the project, more in-depth analysis and further experimentation will be carried out using these ‘in-house’ models. After describing the models we show how the models simulate the climate of the present day (or recent past), focusing on impacts-relevant basic measures, and comparing where possible with observations. Following on, we show the CMIP5 multi-model projections of change in Amazonia. Finally, we focus on the role of the RCP land use change in the projections of change, and based on the results, we draw conclusions on the suitability of these scenarios for Amazonia and set out recommendations for further research.

## 2. Description of RCP storylines

The CMIP5 climate modelling protocol considers four scenarios describing the evolution of anthropogenic drivers of climate, which are further used to force global climate models (GCMs). These scenarios include fossil fuel emissions, atmospheric concentrations of greenhouse gases (GHGs) –and of other reactive gases– and land-use trajectories (Moss et al. 2010). The Representative Concentration Pathways (RCPs) are four scenarios selected from several different scenarios produced by interdisciplinary modelling frameworks and in contrast to other sets of scenarios (e.g. SRES) they account for climate mitigation policies. The four RCPs characterise therefore a range of potential scenarios of human activities and mitigation strategies, describing pathways of radiative forcing (RF) and equivalent GHGs, in addition to land-use change (van Vuuren et al. 2011). GHG concentrations (Figure 4) and fossil fuel emissions are provided to either force GCMs or to be used in fully coupled (carbon-climate) simulations.

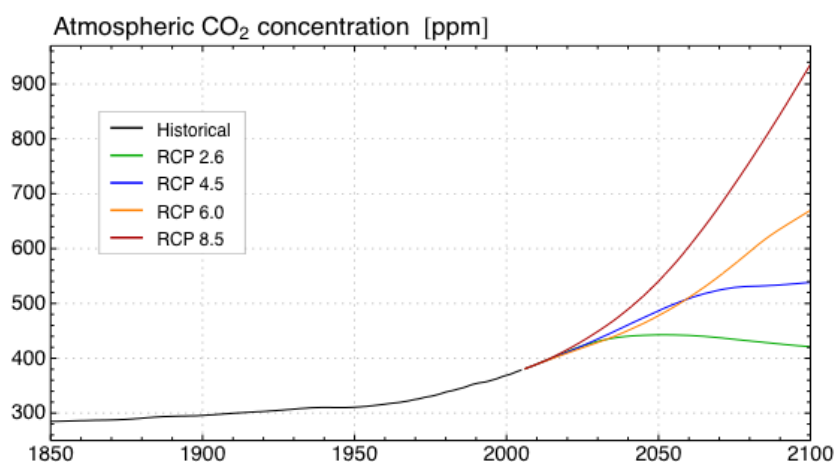


Figure 4. Annual mean atmospheric CO<sub>2</sub> concentration used in CMIP5 concentration-driven simulations for the historical period and future scenarios (RCPs).

An overview of the RCPs is given in Table 1. RCP 2.6 is the pathway chosen from a number of mitigation scenarios, and leads to a limit on global warming of around 2 °C. In this case, the global RF should not exceed 3 W m<sup>-2</sup> and decline to ~2.6 W m<sup>-2</sup> in the 2100 horizon. The

associated change in land-use is the strongest in terms of cropland expansion, in part due to an enhanced development of the biofuel industry, allowing reduced fossil-fuel emissions. RCP 4.5 is a medium-to-low stabilization scenario that leads to a limit in the RF of  $\sim 4.5 \text{ W m}^{-2}$  by 2100. In this case, land-use changes include extensive reforestation as part of a carbon mitigation strategy. Crop areas decline and improvements in yield production and trade are taken in account to satisfy the increasing food demand. RCP 6.0 is the third stabilization scenario in which RF is limited to  $\sim 6 \text{ W m}^{-2}$  by 2100. Agriculture expands worldwide following the food and energy demand, but this occurs mainly to the detriment of pre-existing grasslands with moderate changes in forest cover. RCP 8.5 represents the non-climate policy (business as usual) scenarios. This has an associated RF of  $\sim 8.5 \text{ W m}^{-2}$  and a rising trend towards 2100. In this case, croplands and pasturelands continue to expand at current rates, notably in developing countries, resulting in the largest deforestation scenario of the four RCPs discussed.

A gridded land-use dataset to be used in climate models (e.g. continuous in time and space) was developed from the four RCPs. The latter were post-treated and integrated in a coherent way along with the historical agricultural information provided by HYDE 3.1 (Goldewijk et al. 2011). The resulting dataset, referred to as Land-Use Harmonization (LUH) (Hurtt et al. 2011), includes annual maps of agricultural (crops and grazed lands), urban, primary and secondary land data from 1500 to 2100, in addition to the underlying transition between these land-cover units, wood harvest and shifting cultivation.

Table 1. Representative Concentration Pathways (RCPs) summary.

Scenario (IAM)	Radiative forcing pathway <sup>a</sup>	LULCC <sup>b</sup>	Reference
RCP 2.6 (IMAGE)	Peak in radiative forcing at $\sim 3 \text{ W/m}^2$ ( $\sim 490 \text{ ppm CO}_2$ equivalent) before 2100 and decline to $2.6 \text{ W/m}^2$ by 2100.	Mitigation scenario. High cropland expansion in part due to biofuels demand.	Van Vuuren et al. (2011b)
RCP 4.5 (GCAM)	Stabilization without overshoot pathway to $4.5 \text{ W/m}^2$ ( $\sim 650 \text{ ppm CO}_2$ equivalent) at stabilization after 2100.	Stabilization scenario include reforestation in NH. Food demand is basically achieved through yield improvements.	Wise et al. (2009)
RCP 6.0 (AIM)	Stabilization without overshoot pathway to $6 \text{ W/m}^2$ ( $\sim 850 \text{ ppm CO}_2$ equivalent) at stabilization after 2100.	Cropland expansion due to food and energy demand, mainly to the detriment of grassland.	Fujino et al. (2006)
RCP 8.5 (MESSAGE)	Rising radiative forcing pathway leading to $8.5 \text{ W/m}^2$ ( $\sim 1370 \text{ ppm CO}_2$ equivalent) by 2100.	Strong increase and weak decrease in cropland areas in developing and developed countries, respectively.	Riahi et al. (2007).

<sup>a</sup> Adapted from van Vuuren et al. (2011)

<sup>b</sup> See Hurtt et al. (2011)

Figure 5 shows the pathways of the global cropland extent between 1850 and 2100, as well as the geographical distribution of the differences in crop area between the ends of the historical period (2005-1850) and future scenarios (2100-2006). Between 1850 to 2005 cropland increases globally from  $\sim 5$  to  $\sim 15$  million  $\text{km}^2$ , consistent with what is reported from HYDE 3.1 (Goldewijk et al. 2011), and it continues to expand into the future for the three scenarios: RCPs 2.6, 6.0 and 8.5 (Figure 5a). The largest crop increases take place in the mitigation scenario (RCP 2.6), reaching  $\sim 20$  million  $\text{km}^2$  in 2100. In contrast, crop area decreases in the RCP 4.5 case, reaching 11 million  $\text{km}^2$  in 2100.

During the historical period, land conversion is particularly intensive in the northern mid-latitudes, notably in the North American Great Plains, with an extensive area showing changes in land-cover fractions larger than 50% (Figure 5b). Although comparable to the global totals, the future land-use scenarios do not show extensive regions with land conversion as large as those observed during the historical period, and few localized regions show fractional vegetation changes larger than 25% between 2000 and 2100.

How much the evolution of cropland and grazing land (from datasets such as LUH) affects the forest extent will largely depend on the strategy adopted to incorporate land-use information into e.g. the land-cover maps of a given land surface model (LSM). This issue has been discussed within the LUCID intercomparison project and represents a major source of uncertainty in the simulated climate impacts of land-use changes (Boisier et al. 2012; Brovkin et al. 2013 *in revision*; de Noblet-Ducoudre et al. 2012).

For instance, RCPs 2.6 and 8.5 show the strongest disturbances at low latitudes (Figure 5c, f), but the resulting deforestation concerns areas of mixed vegetation (open forest and savannas), such as in the sub-Sahel zone or in eastern tropical Africa, and do not affect rainforest particularly. This does not correspond either with the observed forest clearing during the last decades or with the regional-scale projections of land-use change that foresee stronger pressure over tropical forest, notably in the Amazon (see Figure 22).

The cropland evolution in RCP 4.5 towards 2100 shows a general picture that roughly inverts the historical LULCC (Land Use/Land Cover Change) pattern, going back to the state of the mid-20th century (Figure 5d). In the case of RCP 6.0, cropland continues to expand in regions already modified during the historical period (Figure 5e).

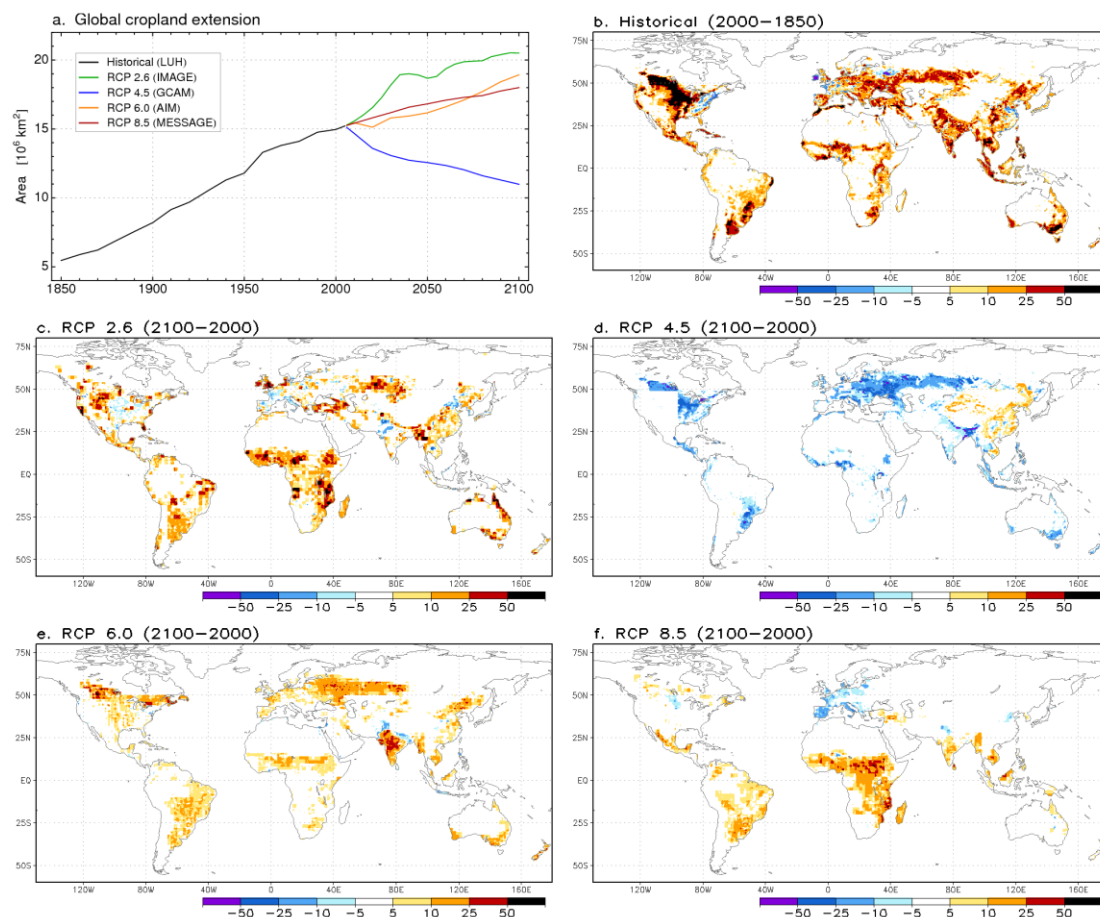


Figure 5. Global cropland area between 1850 and 2100 based on the LUH dataset (a). Maps indicate the difference in the crop areal fraction between the first and the last year of the historical period (2005–1850; b) and of the future scenario period (2100–2006) based on RCP2.6 (c), RCP4.5 (d), RCP6.0 (e) and RCP8.5 (f).

For the projections reported on here, we focus on RCP8.5 as representative of a high-end, ‘business as usual’-type scenario, RCP4.5 as a mid-range scenario in terms of radiative forcing but which also has very different land-use change, and RCP2.6 as a mitigation scenario.

### 3. Description of models

In AMAZALERT, we take advantage of the state-of-the-art in climate modelling to provide projections of change in Amazonia. The Fifth Assessment Report of the Intergovernmental Panel on Climate Change (IPCC AR5), to be published in 2014, will report on simulations that have been carried out through the Coupled Model Intercomparison Project phase 5 (CMIP5). For this Deliverable, we set out the CMIP5 projections of change for Amazonia, and highlight the results given by two of the models from AMAZALERT partners Met Office and IPSL. These are highly complex Earth system models and will be used for more in depth analysis and additional experiments during the course of the project. In this section, we first provide a general overview of the CMIP5 ensemble before describing in detail the Met Office model HadGEM2-ES and the IPSL model IPSL-CM5A.

## CMIP5 ensemble

Scientific uncertainties are inherent in any projections of climate, and these are derived from several sources. An important way to explore the implications of uncertainties on the projections of change is to use a group of models, or 'ensemble'. Take, for example, the emissions pathway: running a climate model under the RCPs demonstrates the simulated effects of different forcing according to differently evolving greenhouse gases. Even given the same forcing, between-model differences can be significant, particularly at the regional scale, and particularly for important variables such as the components of the water cycle. One method for characterising this type of modelling uncertainty in projections of future change is to assess those changes in a number of different models. By conducting the same experiment with an ensemble of different models, the range in model response can be explored.

In AMAZALERT we take advantage of the state-of-the-art in ensemble model projections of climate change available through the CMIP5. CMIP5 comprises a coordinated suite of experiments run by climate modelling groups around the world. These experiments have been designed to address a number of research priorities towards improving understanding of past and future climate change, comparing and assessing model behaviour and exploring model capabilities (Taylor et al. 2012). In addition, efforts to coordinate the requirements for model output have resulted in a commitment to archive a more comprehensive list of variables available to researchers for analysis (Taylor et al. 2012). Model output is being stored in archives managed by the Project for Climate Model Diagnosis and Intercomparison (PCMDI). Core experiments under the CMIP5 protocol are the long term (centennial scale) integrations and form the basis of the multi-model projections of change in Amazonia presented in this report. These long term experiments build on those of previous CMIP phases by employing the latest models driven by updated forcing scenarios (RCPs, described in Section 2).

Generally, the set of climate models included within CMIP5 have a higher spatial resolution than those in CMIP3, and many modelling centres have increased the complexity in their models. Some (including HadGEM2-ES and IPSL-CM5A) should more properly be termed Earth System Models (ESMs), and permit potentially important feedbacks between the different components of the earth system. There is no strict definition of the point at which a climate model becomes an ESM, but it is generally accepted that an ESM should include the terrestrial and marine carbon cycles (Collins et al. 2011). The benefits of including earth system components means that, for example, the impacts of climate change on terrestrial or marine ecosystems can be directly simulated, without the requirement for offline impacts modelling, so keeping things internally consistent. In addition, it permits feedbacks between the different earth system components, which may act to amplify or dampen the original effects.

## HadGEM2-ES

HadGEM2-ES (Collins et al. 2011) is an Earth System Model (ESM) of the Met Office Hadley Centre's Global Environmental Model version 2 (HadGEM2) family (Martin et al. 2011). The atmospheric component has a horizontal resolution of  $1.25^\circ$  latitude  $\times$   $1.875^\circ$  longitude with 38 levels in the vertical. The ocean has a horizontal resolution of  $1^\circ \times 1^\circ$ , the meridional component of which increases smoothly in the tropics to  $1/3^\circ$  at the equator, and 40 vertical levels. Figure 6 is a schematic of how different components of the earth system in HadGEM2-ES are coupled.

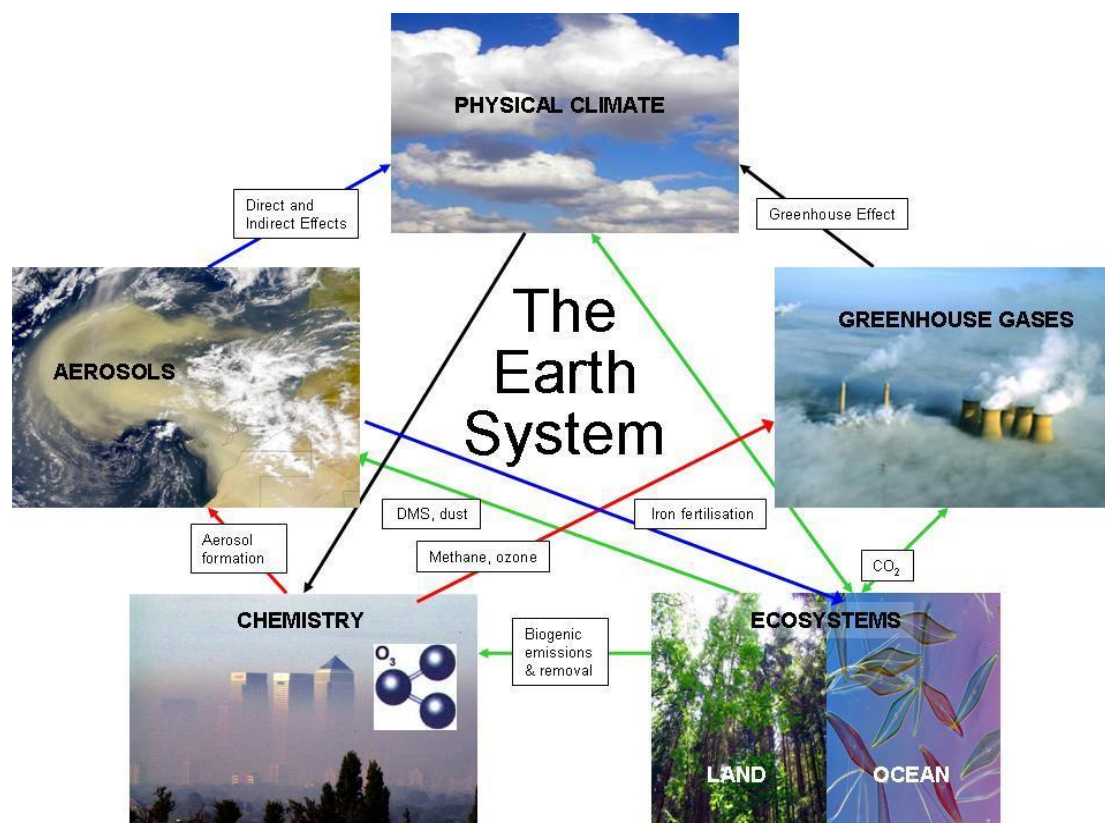


Figure 6. Couplings in the Earth System. Collins et al. (2011), their Figure 3.

In HadGEM2-ES, land surface processes including plant physiology and the surface energy and moisture budgets are simulated with the 2nd version of the Met Office Surface Exchange Scheme (MOSES II; Essery et al, 2003). Some improvements have been made compared to previously published versions of MOSES II in order to improve the simulation of global carbon cycle processes (Collins et al. 2011), including improved representations of deep soil moisture (Clark and Gedney 2008), wetlands (Gedney et al. 2004), and penetration of light into vegetation canopies (Mercado et al. 2009). MOSES II also includes large scale vegetation dynamics simulated by TRIFFID (Cox 2001) – the global patterns of vegetation are simulated within the Earth System Model, with vegetation represented by 5 plant functional types (PFTs): broadleaf tree, needleleaf tree; C3 grass; C4 grass; and shrub. These PFTs are subject to competition rules and the net carbon uptake of each PFT simulated within the land surface scheme is closely coupled with the water budget.

Natural disturbance to the vegetation is prescribed by a uniform disturbance rate – there is no representation of the effects of climate on disturbance regimes such as fire, windthrow, disease or insect attack, and neither is there any explicit representation of herbivory. Tropical forests of South America and Africa extend slightly too far into savanna regions – this may be because fire disturbance is not included in the model. The implicit assumption in the model is that natural disturbance regimes remain constant over time. This may be a limitation of the model when used in climate change studies (Betts et al. 2013 *submitted*). Anthropogenic land use, such as in the RCPs, is simulated through the imposition of a “Disturbed Fraction” which designates a specific fraction of the gridbox as unavailable to tree and shrub PFTs – all agricultural land including croplands is therefore represented as either C3 or C4 grass, depending on which is simulated to grow best under local climate conditions.

The physical properties of the land surface, such as albedo, aerodynamic roughness, and factors affecting moisture availability for evaporation, are directly affected by the PFT

distribution and the simulated Leaf Area Index (LAI) of each PFT and the fractional cover and physical properties of the ice, water and bare soil portions of the gridbox. This means that changes in vegetation cover directly influence the climate through the surface energy and moisture budgets.

A key feature of the model is that terrestrial ecosystems and hydrology are tightly coupled. Changes in vegetation cover, whether in response to climate change or anthropogenic land use, affect surface evaporation and transpiration rates, with consequent implications for soil moisture and runoff. Vegetation responses to increasing CO<sub>2</sub> concentrations also affect the hydrology through changes in transpiration. Some studies have found that higher CO<sub>2</sub> concentrations result in decreased transpiration and increased runoff (Betts et al. 2007) but uncertainties in these responses are perhaps larger than previously discovered (Davie et al. 2013 *in open review*). Total runoff is routed to the oceans using the TRIP global river model (Oki and Sud 1998), which simulates river flows through a network resolved on a 1° × 1° grid. The simulations of terrestrial ecosystem distribution and river flows in HadGEM2-ES are therefore fully consistent with each other and with the overlying climate.

## IPSL-CM5A

IPSL-CM5 is the fifth generation climate model of the *Institut Pierre Simon Laplace* (IPSL) climate-modelling framework. In a fully coupled configuration, the model aggregates physically and chemically based schemes of the atmosphere, the land and the ocean. The base components of IPSL-CM5 are the atmospheric global circulation model LMDZ (Hourdin et al. 2012) and the ocean one NEMO (Madec 2008), in addition to the land surface model ORCHIDEE (Krinner et al. 2005). The land and ocean biochemistry are computed with STOMATE and PISCES (Aumont and Bopp 2006), modules of ORCHIDEE and NEMO, respectively. The tropospheric and stratospheric chemistry are treated in INCA and REPROBUS, both modules built in LMDZ.

Major model improvements from the version used in the CMIP3 (IPSL-CM4) concern the atmospheric chemistry and the carbon cycle. A new set of physical parameterizations for atmospheric processes was also developed (Hourdin et al. 2012), but is included in a parallel version of the model (IPSL-CM5B). The resolution was also enhanced from that used in CMIP3. The set of CMIP5 simulations were carried out with a horizontal resolution of 1.875° × 3.75° and 39 vertical levels. For an in-depth description of IPSL-CM5, see Dufresne et al. (2013 *accepted*) and references therein.

ORCHIDEE builds on the energy and hydrologic transfer model SECHIBA (Ducoudré et al. 1993) and use two other schemes that respectively simulate plant biogeochemistry (STOMATE) and vegetation dynamics (LPJ; Sitch et al., 2003). Hence, this model has a modular architecture that allows using it in a SECHIBA configuration alone, in a SECHIBA-STOMATE configuration or in a fully coupled configuration, in which ORCHIDEE works as a DGVM. When STOMATE is activated, the carbon cycle is integrated to the biophysical component in a coherent manner; the model simulates photosynthesis, stomatal conductance and autotrophic respiration following Ball et al. (1987), Farquhar et al. (1980), Collatz et al. (1992) and Ruimy (1996). STOMATE accounts for carbon allocation into the different vegetation pools (and into the litter and soil ones in regard with leaf senescence and tree mortality), plant phenology, litter decomposition and the soil carbon dynamics. The global biogeography and the sub-grid land-cover distribution are characterized through twelve PFTs living within a grid-cell, in addition to a bare soil class. There are six tree and four herbaceous PFTs, the latter including two (C3 and C4) crop- and grass classes.

For CMIP5 simulations, land-use change was taken into account in ORCHIDEE by following a similar protocol as the one used in the first phase of the LUCID intercomparison project (de

Noblet-Ducoudré et al., 2012). The method basically consists of two steps, applied every year from 1700 to 2100 over the natural vegetation map currently in use in ORCHDEE (this is based on satellite data by Loveland et al. (2000)). First, crop grid areal fraction from LUH (Hurtt et al. 2011) dataset is prescribed as the two specific crop PFTs (C3 and C4). At this stage, the natural vegetation (8 trees and 2 -C3/C4- grass PFTs) is proportionally reduced to allocate crops. Given that pastures are described as natural grasses in ORCHIDEE, the second step increases grass PFTs fractions at expense of those of forest and bare soil only if the grazed land fraction given by LUH is larger than the ORCHIDEE grass fraction resulting in the first step. Therefore, the resulting vegetation maps replicate cropland extension and evolution provided by LUH, while grass and forest areas could either increase or decrease depending on the crop area and grazed land evolution provided by LUH, and the background land-cover map used.

## 4. Baseline validation

Comparing, where possible, the model climate with observations, is an important step in demonstrating some of the model biases, it gives pointers towards areas where the model performs well or badly in the simulation of important processes, and it informs the interpretation of the future projections. At this stage, there is no formal effort to rank models according to ability to simulate the climate. Developing metrics for the ranking of models is complex and not uncontroversial. Moreover, in the Amazon region, data are relatively very sparse and hence there are uncertainties too in what constitutes the true state and historical variations. Here, we compare with observations some important aspects of the baseline (late 20<sup>th</sup> century) climate, including means and teleconnections with relevant patterns of climate variability.

### Mean state and seasonal cycle

There is a fairly narrow spread in the representation of temperature in the Amazon basin by the CMIP5 models, with some simulating warmer and others cooler than the observations, provided by CRU TS3.0 (Figure 7a). In basin scale temperature, there is no clearly defined seasonal cycle. By contrast, the seasonal cycle in precipitation is strong, and changes in the dry season have been put forward as potentially being of key importance to future forest health. CMIP3 models were reported to substantially underestimate rainfall over Amazonia almost across the board (Malhi et al. 2009). This introduces difficulties in the interpretation of simulated changes, particularly in cases where thresholds in absolute rainfall are important.

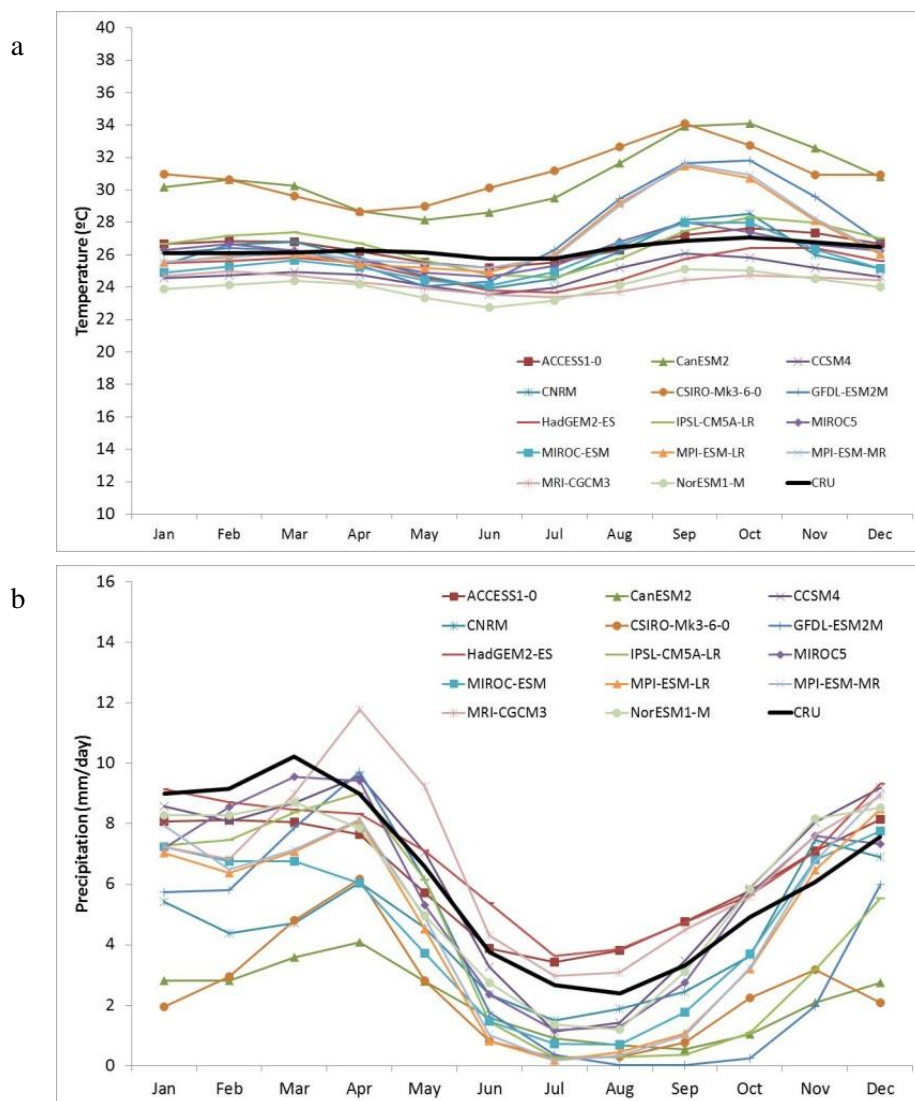


Figure 7. Climatological seasonal cycle of temperature (a) and precipitation (b) over the Amazon region in the late 20<sup>th</sup> century: CMIP5 simulations (coloured lines) and CRU observations (black line).

Although the seasonal cycle of rainfall is reasonably well captured by this subset of CMIP5 models, the simulated magnitude generally remains quite poor (Figure 7b). The majority of the models simulate deficient rainfall in comparison with the observations, in a similar way as the CMIP3 models. However, a few models do have rainfall totals closer to the observations, and some are even a little wetter. One of these is HadGEM2-ES, which tends to underestimate summer wet season rainfall but slightly overestimates rainfall during the remainder of the year. This represents a significant change from the previous generation of Met Office models (HadCM3), which tended to be much drier than the observations over Amazonia.

Mapping the bias in the baseline precipitation for the wet (DJF) and the dry (JJA) seasons (Figure 8) shows the spatial expression of the bias.

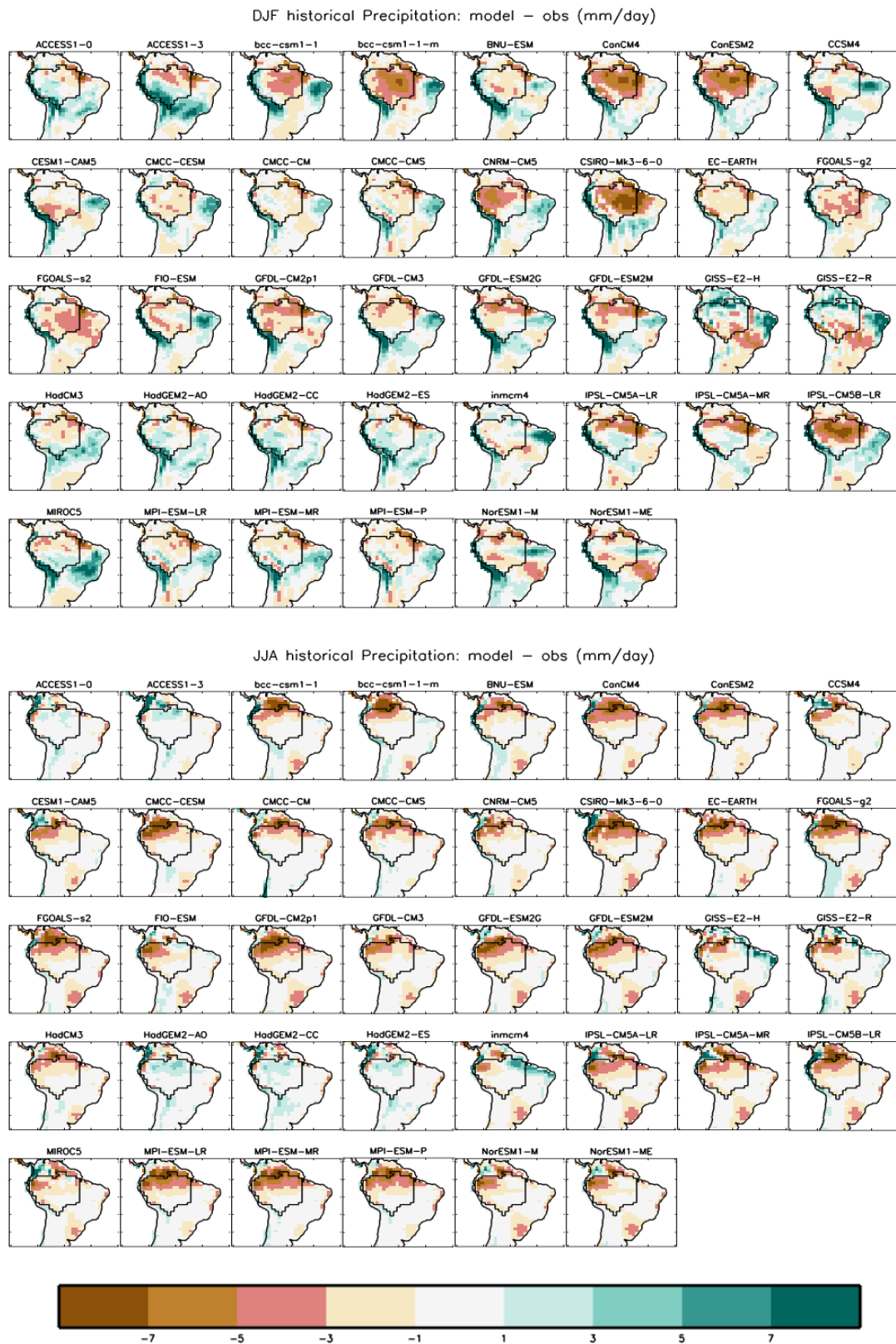


Figure 8. Difference between modelled and CRU TS 3.1 observed precipitation ( $\text{mm day}^{-1}$ ) for DJF (top) and JJA (bottom). Brown colours indicate that the model is drier than the observations and green colours that it is wetter.

### **Teleconnections with the tropical Pacific and Atlantic**

Tropical sea surface temperatures (SSTs) are recognised as among the main drivers of precipitation trends and variability on a range of timescales, both in Amazonia and throughout the tropics (e.g. Ropelewski and Halpert 1987; Liebmann and Marengo 2001; Ronchail et al. 2002; Marengo 2004; Marengo et al. 2008; Yoon and Zeng 2010; Marengo et al. 2011b). Through atmospheric teleconnections, the influence of SST anomalies can be felt at remote locations.

The most well-known mode of tropical SST variability is the El Niño Southern Oscillation (ENSO), which has its centre of action in the Pacific. During warm-phase ENSO – El Niño – a large portion of tropical South America experiences reduced rainfall, including east-northern Amazonia, while the opposite conditions tend to occur during the reverse phase – La Niña (Aceituno 1988; Marengo 1992). The severe droughts of 2005 and 2010 on the other hand have been related to a SST gradient in the tropical Atlantic (Cox et al. 2008; Marengo et al. 2008; Espinoza et al. 2011; Marengo et al. 2011b). The SST gradient between the north and south tropical Atlantic has influence over the position of the Inter-tropical Convergence Zone (ITCZ: a latitudinal band of convergence, ascent and precipitation that migrates seasonally). When SSTs are higher than usual in the northern tropical Atlantic relative to the south, rainfall is reduced over Amazonia. This teleconnection is particularly important during the late dry season when rainfall deficiencies can have much larger impacts than during the wet season (Marengo et al. 2011b).

Given the significance of tropical Pacific and tropical Atlantic SSTs for Amazonian precipitation, it is instructive to examine the ability of the CMIP5 models to capture these relationships. Moreover, it is a step towards a more robust evaluation of models against observations.

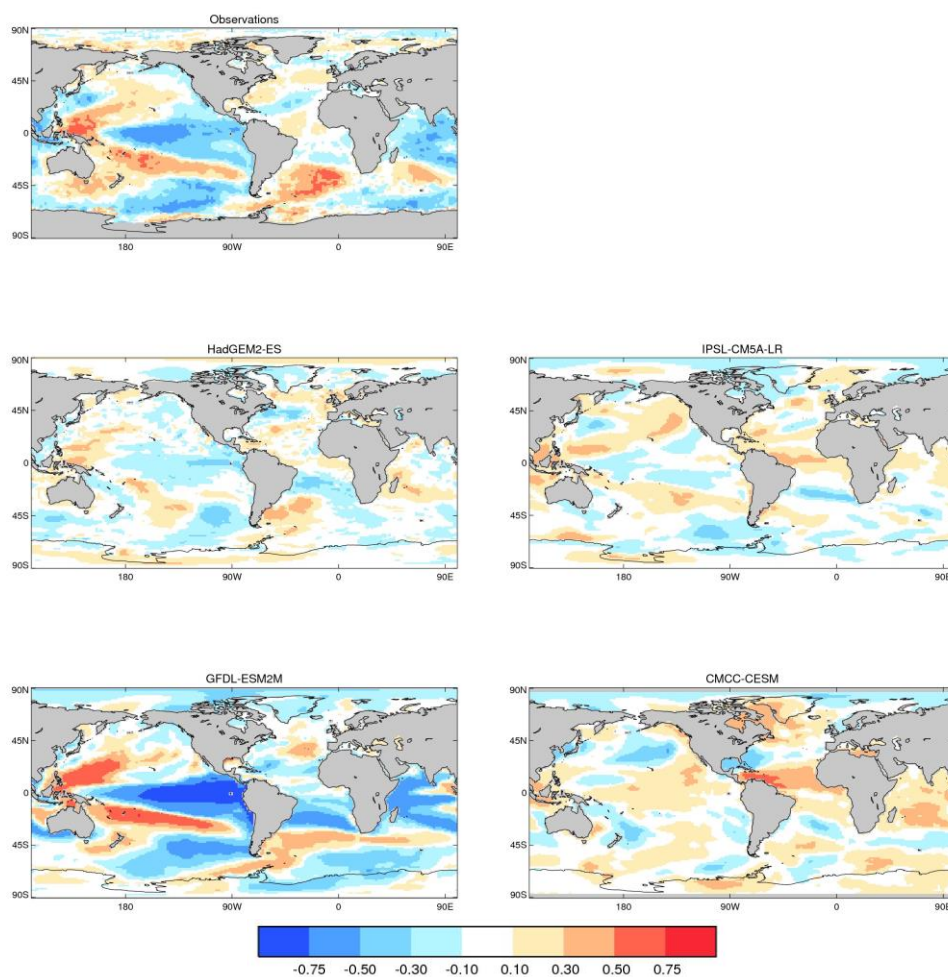


Figure 9. Maps of spatial correlation between precipitation averaged over Amazon Basin and global SSTs for observations (CRU precipitation and HadISST) and selected CMIP5 models (precipitation and SSTs) for the period 1961 to 2000 December-January-February. All data are detrended.

In austral summer (DJF), the pattern of correlations between observed Amazon basin precipitation and Pacific Ocean SSTs have an ENSO signature, with the sign of the correlation indicating that El Niño events are associated with drier conditions in Amazonia (Figure 9). Comparison with model SSTs and precipitation from CMIP5 historical runs shows that many but not all of the models are able to reproduce the salient features. Of the 32 CMIP5 models analysed here, twelve exhibit ENSO-type correlation patterns in approximately the same regions as the observations but of weaker magnitude, e.g. HadGEM2-ES and IPSL-CM5A-LR. There are others in which the tropical Pacific area of negative correlation is stronger than in observations, e.g. GFDL-ESL2M (Figure 9), but in some models the Pacific correlation pattern is largely absent and of incorrect sign, e.g. CMCC-CESM (Figure 9). The JJA correlation pattern in observations is similar to the DJF pattern in the Pacific but includes a dipole in the tropical Atlantic (Figure 10), thought to play an important role in dry season drought (Cox et al. 2008; Good et al. 2008; Harris et al. 2008). The dipole is captured in 26 out of 32 models, including IPSL-CM5A-LR and HadGEM2-ES but it is absent in 6 models, e.g. MPI-ESM-LR and MPI-ESM-MR.

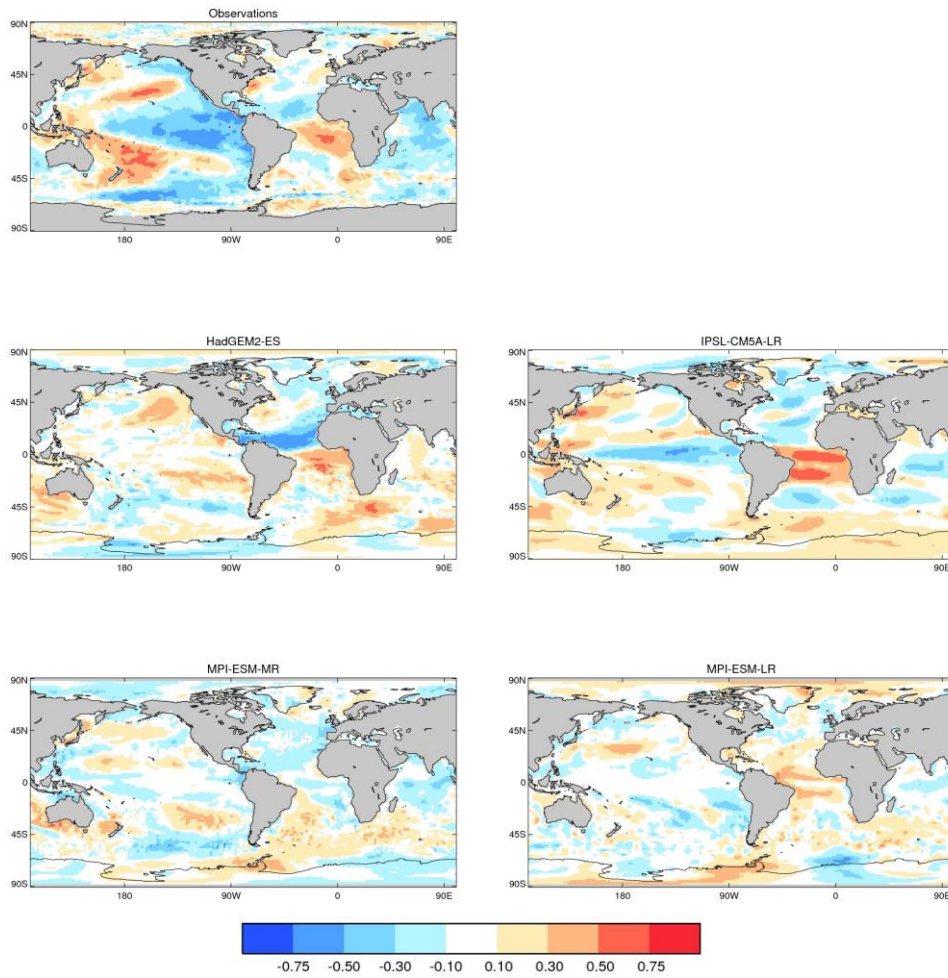


Figure 10. As Figure 9, but for JJA.

In order to examine the relationships throughout the seasonal cycle, Amazon basin precipitation was correlated with ENSO SST index Niño3.4 (Figure 11) and tropical Atlantic gradient SST index TAG (Good et al. 2008) (Figure 12).

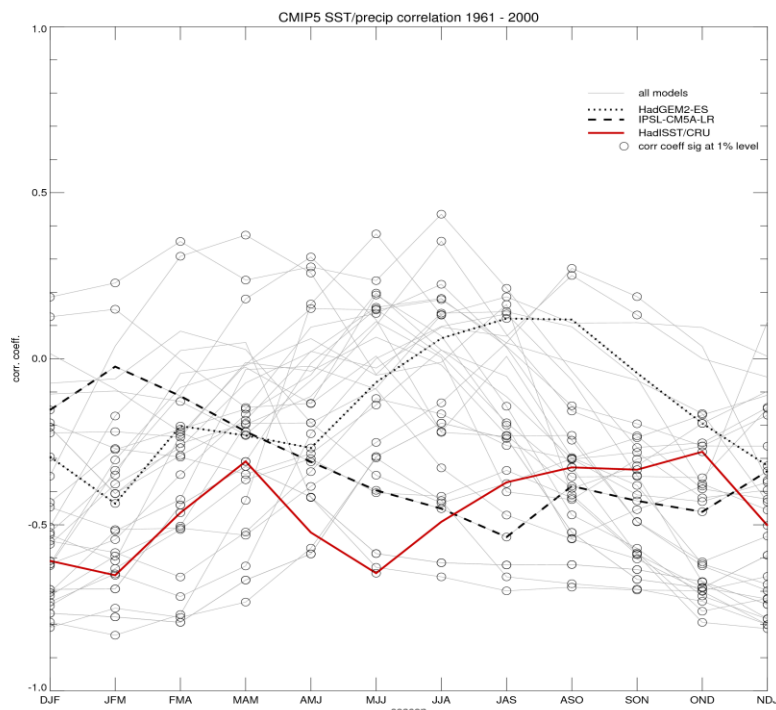


Figure 11. Correlation between precipitation averaged over Amazon Basin and ENSO index (Nino3.4) for observations (CRU precipitation and HadISST) and CMIP5 models (precipitation and SSTs) for each season in the period 1961 to 2000. All data have been detrended. Month names are abbreviated to their initial letter, and are considered in 3-month seasons.

It is striking that for ENSO, the models do not follow the seasonal cycle of the observations (Figure 11). There is a broad consensus towards positive correlation in JJA and negative in the other seasons but observations show negative correlation throughout the year. HadGEM2-ES does follow the pattern from OND (Oct-Nov-Dec) to MAM (Mar-Apr-May) but becomes positive in JJA as for the majority of models. In contrast, IPSL-CM5A-LR is more similar to observations from JAS (Jul-Aug-Sep) to OND but does not capture the strong correlations in DJF and JFM.

For TAG, there is much more agreement between models and the observations (Figure 12). The models consistently show a pattern of maximum negative correlation in JJA, with most reverting to a strong positive correlation in DJF to MAM. However, in the observations the maximum negative correlation occurs in ASO, and includes no significant positive correlations. Both HadGEM2-ES and IPSL-CM5A-LR have a much stronger negative correlation in JJA compared to observations, which persists into SON (Sep-Oct-Nov) in IPSL-CM5A-LR, which may have implications for the future interpretation of precipitation projections.

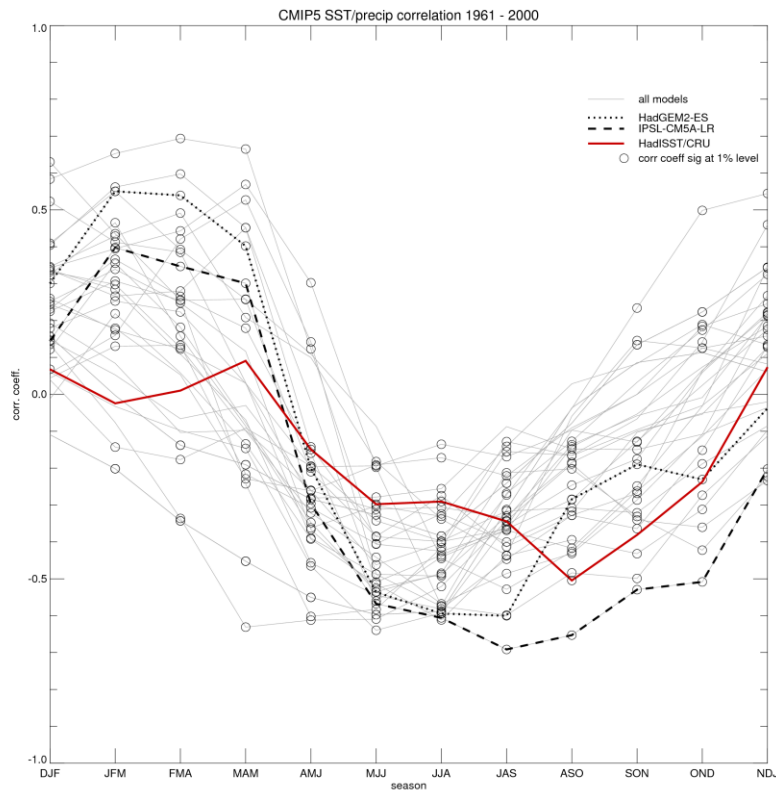


Figure 12. As Figure 11, but for TAG

## 5. CMIP5 historical runs and projections of change in Amazonia

### Projections and seasonality

As concentrations of atmospheric GHGs rise, surface temperatures are likewise projected to increase (Figure 13). The CMIP5 ensemble displays some spread in its projections of change, and until the middle of the century the modelling spread exceeds the difference between the RCPs. However during the second half of the century the level of warming in both summer (DJF) and winter (JJA) become clearly scenario dependent, with the greatest warming under RCP8.5 and the least under RCP2.6.

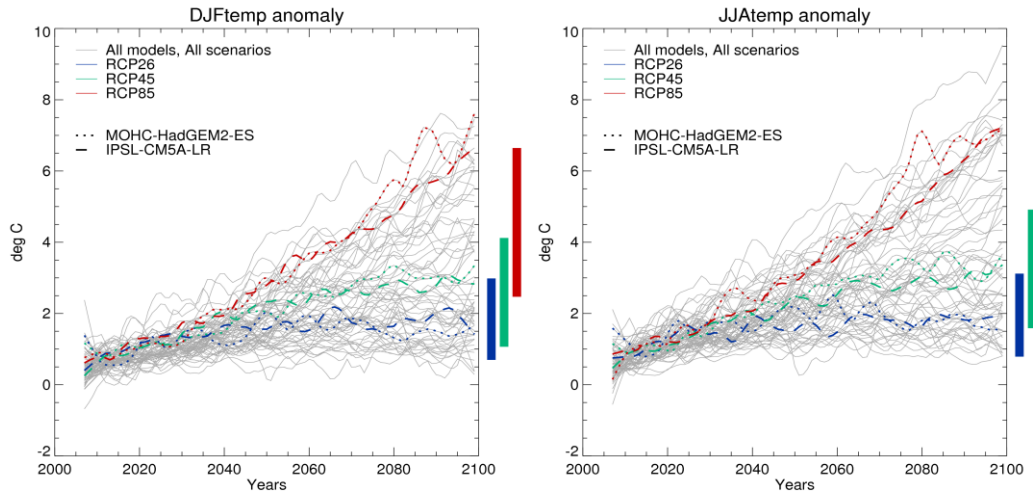


Figure 13. Temperature change (°C) over the Amazon basin relative to the baseline in left: DJF; right: JJA. Grey lines show the evolution of temperature in all models for all scenarios. Projections given by HadGEM2-ES (dotted) and IPSL-CM5A-LR (dashed) are overlaid in colour: RCP2.6 (blue); RCP4.5 (green), RCP8.5 (red). Bars indicate the range in projections according to RCP for the 30-year period 2071-2100 relative to the baseline.

The pattern of warming in the CMIP5 multi-model mean is similar to that displayed by the CMIP3 models (Figure 14). Maximum warming in the South America region occurs over the interior of the continent, including much of Amazonia.

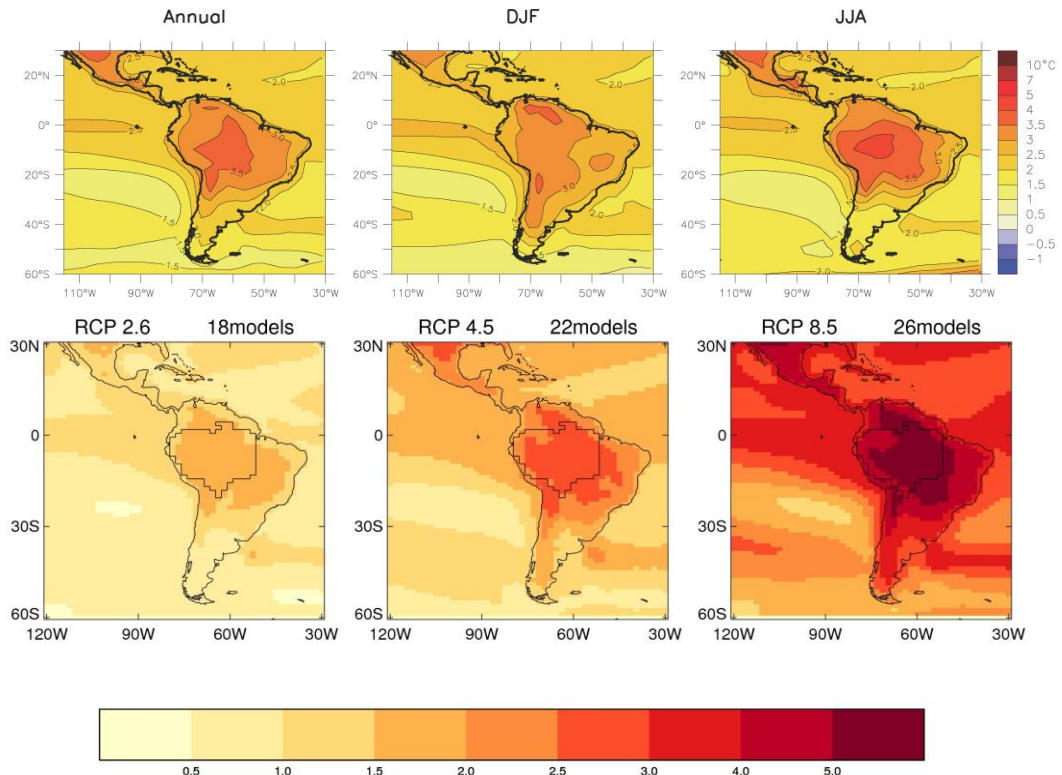


Figure 14. Comparison of CMIP3 and CMIP5 temperature anomaly projections (°C). Top row shows CMIP3 multi-model mean temperature change between late 21st and late 20th centuries under the SRES A1B scenario, as before, their Figure 11.15. Bottom row shows CMIP5 multi-model annual mean anomalies for the three RCPs: 2.6 (left), 4.5 (centre) and 8.5 (right). The number of models contributing to the CMIP5 multi-model mean is marked above each plot.

Projections of precipitation present a more complicated picture (Figure 15). During DJF and MAM, the majority of the models project increases in basin-average precipitation, but the spread of projections span zero, which indicates that some models project drier conditions in the future as well as the majority projecting wetter. In JJA, because of the low rainfall in this season, percentage changes are larger. Although more of the models project a decrease in rainfall during this season, there is a substantial proportion that project increases, including IPSL-CM5-LR. Finally, there is a tendency for a decrease in rainfall during SON, which could signify a move towards a lengthening of the dry season or more prolonged dry season water stress. However, again there is substantial model spread in the projections that spans zero. An important point of difference with the temperature projections is that these rainfall projections are relatively scenario-independent. The bars in Figure 15 show almost complete overlap, although it appears that the spread in the RCP8.5 ensemble is greater than that in RCP4.5 and 2.6.

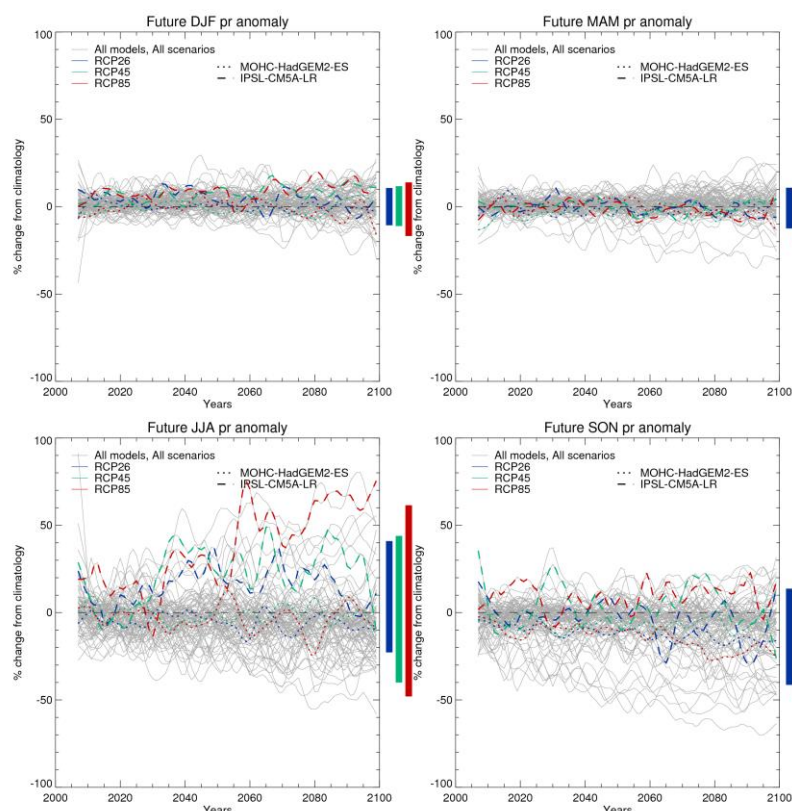


Figure 15. As Figure 13 but for % change in precipitation for each season.

By recreating the IPCC AR4 representation of model ‘consensus’, it is possible to see the spatial expression of the CMIP5 ensemble agreement in the sign and patterns of change (Figure 16). The first thing to note is that the broad-scale patterns of change for DJF and JJA are similar in the CMIP3 and CMIP5 ensembles. Secondly, it is clear that at higher CMIP5 concentration scenarios, there is a greater degree of agreement in the large-scale patterns and sign of change within these. However, if we zoom in on the Amazon basin, there is more of a mixed signal. Generally, there is more model disagreement, as indicated by paler colours, in large parts of northern South America including Amazonia. As the area-average projections suggested (Figure 15), in DJF and MAM there is a tendency towards wetter conditions, although model agreement is low. There is a stronger wet signal in the western basin.

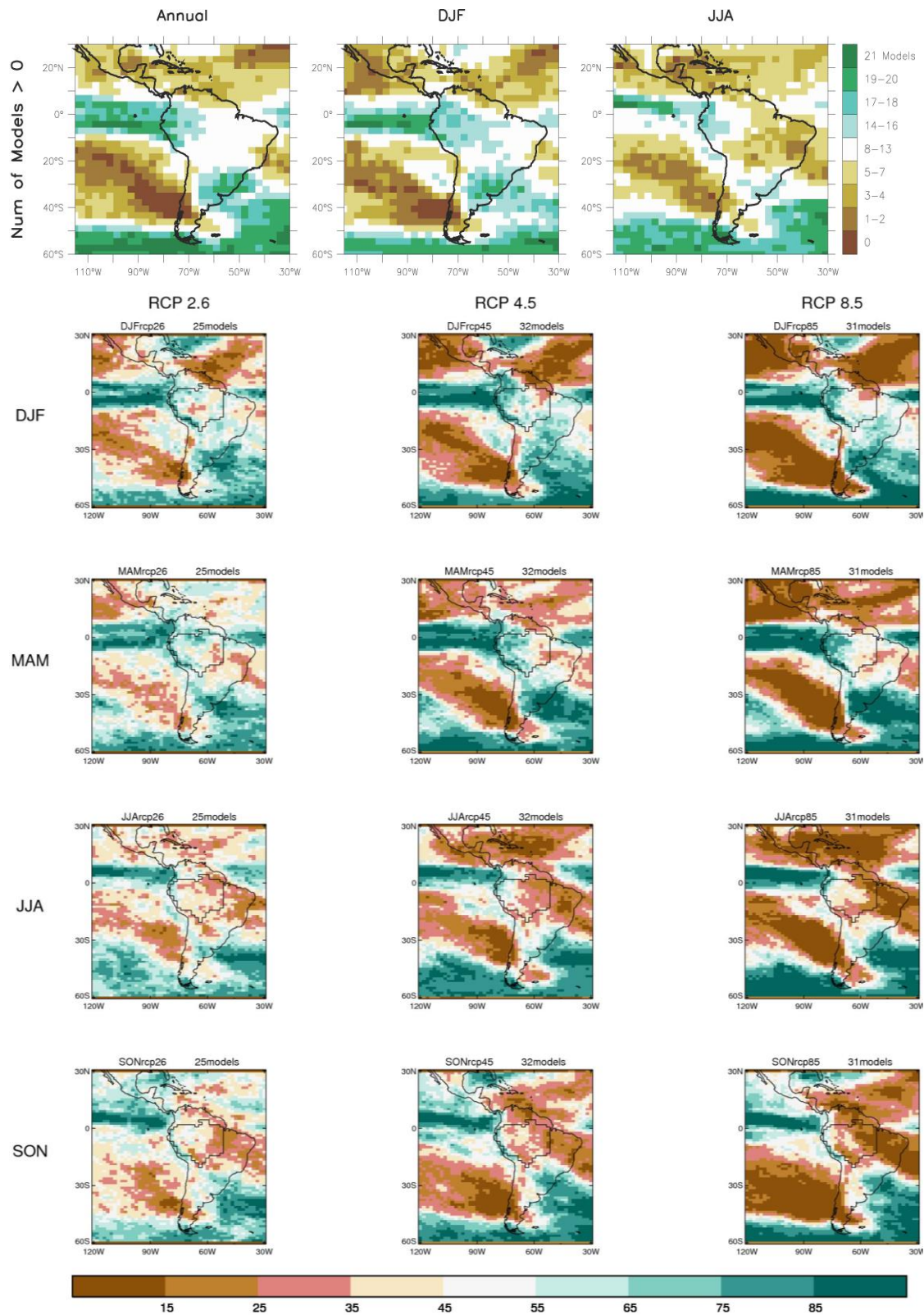


Figure 16. Comparison of CMIP3 and CMIP5 projections: indicator of model consensus in precipitation changes. Top row: CMIP3 as before. Source: IPCC AR4 WGI, part of their Figure 11.15. Bottom four rows: percentage of models that show an increase in precipitation, by season and RCP. Number of models available for each scenario varies according to RCP and is marked above each plot. The Amazon Basin is overlaid. Brown colours indicate model agreement for a drying signal and greens for a wetting signal.

In JJA and more clearly in SON there is greater model agreement for drier conditions, particularly in the eastern basin. The IPCC AR4 (2007) summary of CMIP3 projections of changing precipitation (Figure 1) did not include SON, which is a potentially critical season for the Amazon region.

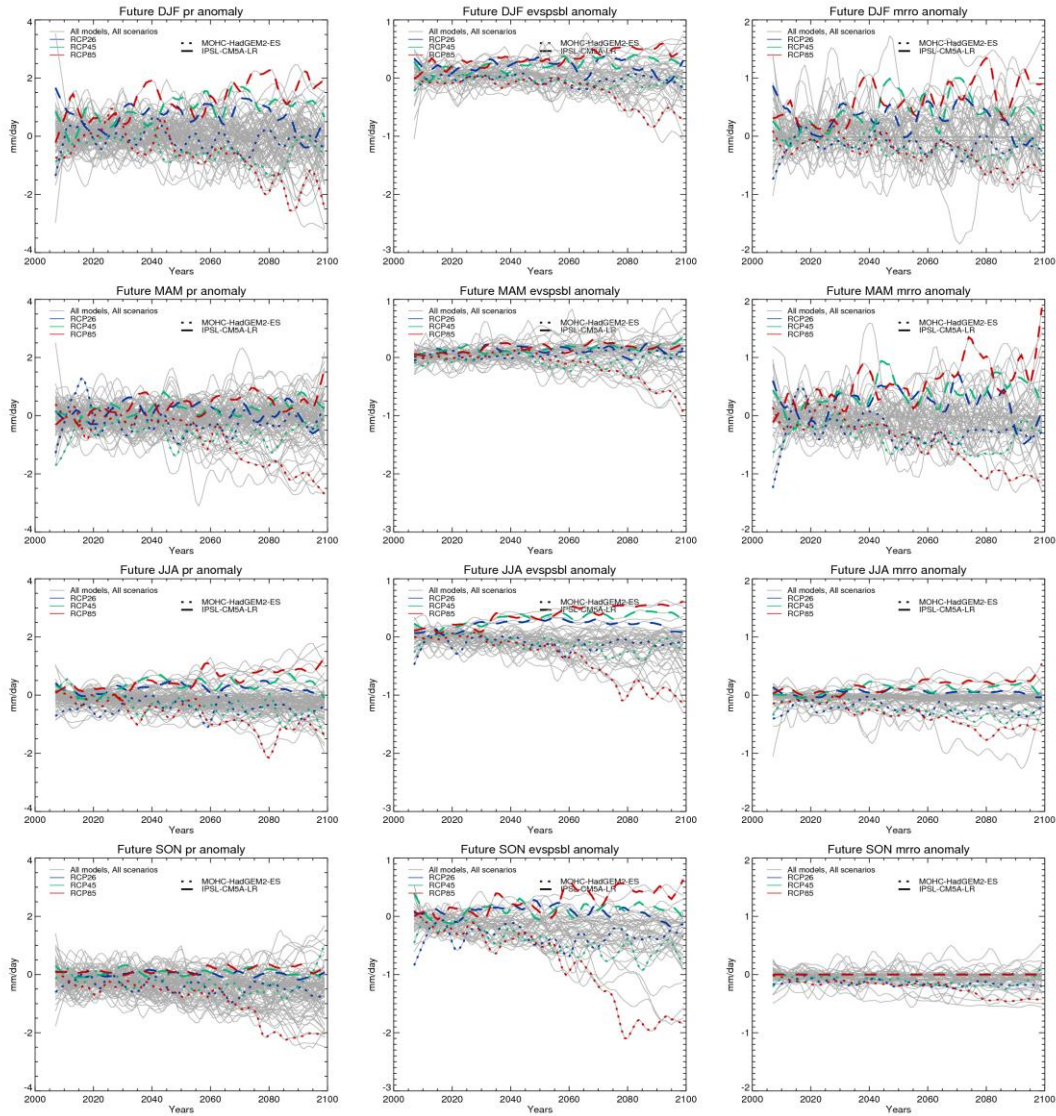


Figure 17. Projections of precipitation (left), evapotranspiration (centre) and runoff (right) anomalies (mm/day) for the eastern Amazon by season.

Looking in greater detail at the eastern Amazon basin, the decreases (increases) in precipitation in HadGEM2-ES (IPSL-CM5-LR) appear to be driving changes of the same sign in runoff. These become more pronounced in the second half of the 21<sup>st</sup> century. Precipitation in IPSL-CM5-LR in SON is very low in the historical period, is outweighed by evapotranspiration, hence leaving no water available as runoff. Changes in the components of the water cycle 21<sup>st</sup> century do not alter this situation, and so future runoff in this season remains at or close to zero. In HadGEM2-ES, evapotranspiration remains fairly constant, decreasing a little until the mid century, when under RCP8.5, there is a sharp decrease in evapotranspiration. This decrease in evapotranspiration is almost of the same magnitude as the reduction in precipitation, and hence runoff does not experience a sharp decline. The large reduction in evapotranspiration is unlikely to be due to changes in land cover, as the simulations with and without 21<sup>st</sup> century land use change (for more details refer to Section 6,

Figure 21) show the same reduction. At this point, there is a change in the partitioning of energy at the surface, with a greater amount being transferred as sensible heat rather than latent heat.

### Future teleconnections with tropical Pacific and Atlantic

Climate change has a direct effect on land and sea surface temperatures through radiative forcing, which then impacts pressure patterns, winds and the hydrological cycle both locally, and through teleconnections, regionally and globally. Uncertainty in the total magnitude of radiative forcing resulting from anthropogenic emissions is reflected in the three RCPs; however, the nature of the teleconnections may not remain constant through time (Collins et al. 2010; Yeh et al. 2009; Yeh et al. 2012), such that a given SST pattern in the present may not have the same impacts in the future. The CMIP5 multi-model ensemble provides an opportunity to investigate the potential evolution of teleconnections in the light of climate change, though it should be noted that such changes may not be externally forced but may instead occur as a result of internal variability. Possible mechanisms for change are not well understood as there is uncertainty in projections of the relative importance of the various feedbacks involved (Collins et al. 2010).

To highlight regions that may experience large changes in teleconnections in RCP 8.5, difference maps for correlation coefficient have been calculated comparing 2061-2100 with 1961-2000. A 40 as opposed to a 30-year period was chosen to increase the robustness of the correlation results.

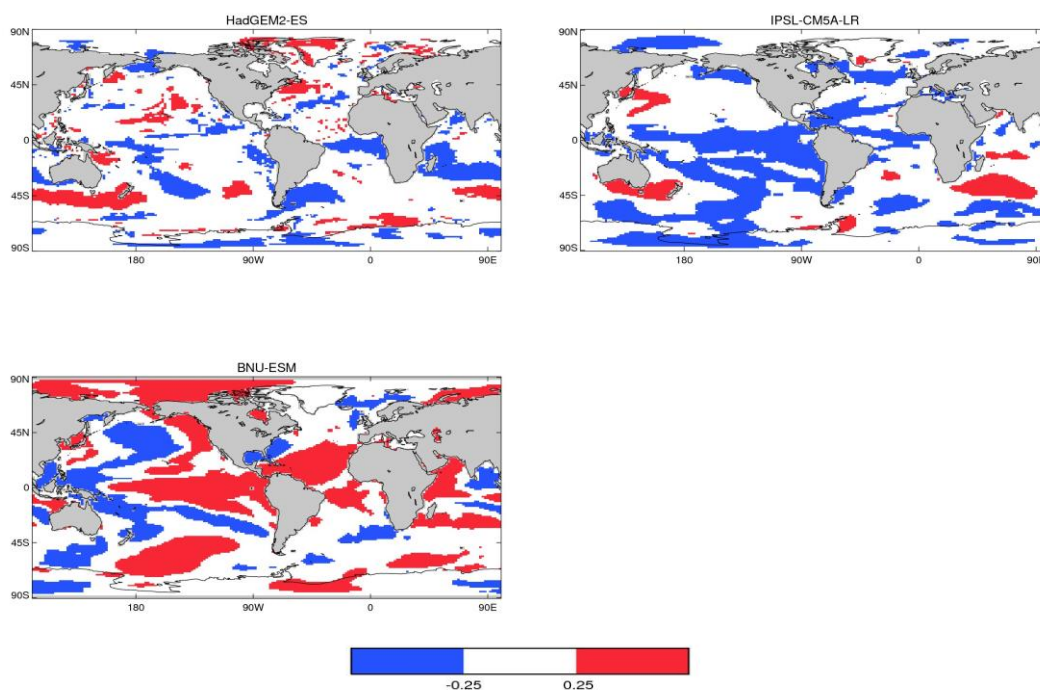


Figure 18. Maps of difference between future minus present correlation of SSTs and Amazon basin precipitation in selected CMIP5 models for RCP 8.5 in DJF.

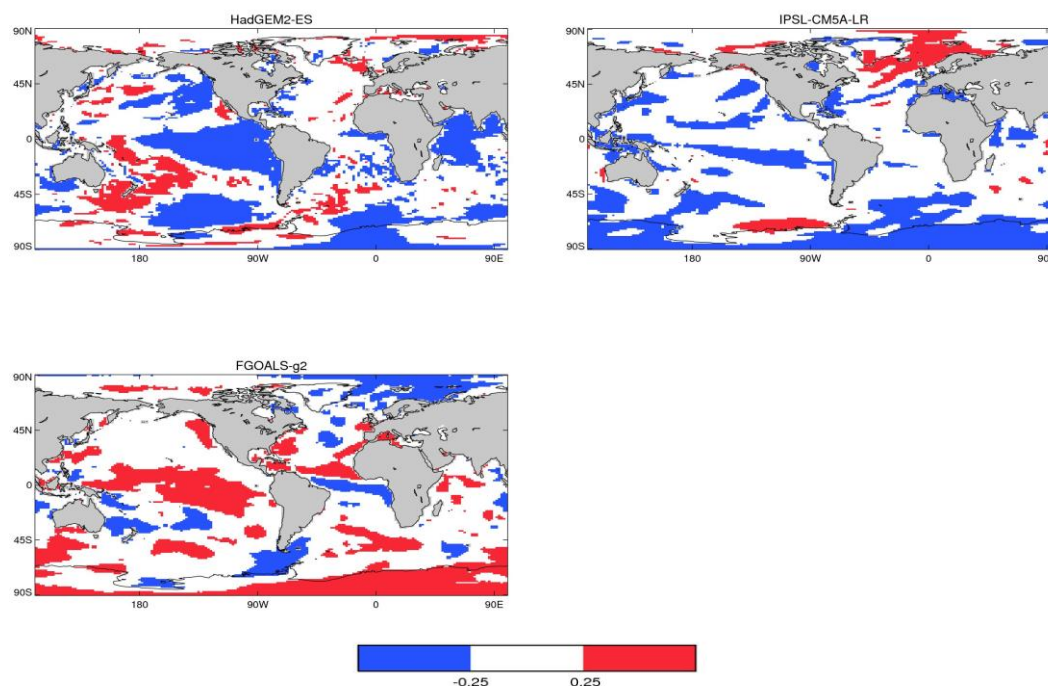


Figure 19. As Figure 18 but for JJA.

The majority of models (16 out of 26) do not indicate large changes in the DJF tropical Pacific correlation patterns (Figure 18), e.g. HadGEM2-ES. However, four models, including IPSL-CM5A-LR, show a more negative correlation, implying a strengthening of the ENSO-Amazon rainfall relationship and four a positive change (i.e. a less negative correlation), e.g. BNU-ESM, implying a weakening of that relationship in the future.

In JJA, we focus on the tropical Atlantic (Figure 19). Around half the models show changes (e.g. FGOALS-g2, Figure 19) but there is little consistency between them; however, HadGEM2-ES and IPSL-CM5A-LR do not show large changes in correlation. This suggests that the relationship with TAG may remain unchanged, which is also implied by the linearity in Figure 20. This is similar to the relationship obtained from IPCC AR4 models (same variables plotted) in Good et al. (2008) though the scenarios are not directly comparable. It shows that Amazon basin precipitation is strongly related to TAG in JJA across models and RCPs. Note that most models project a reduction in precipitation associated with an increase in TAG, as shown by the cluster of points in the lower right quadrant (c. f. Good et al. 2013). This implies that SSTs will increase in the tropical North Atlantic relative to the tropical South Atlantic. A few models, including IPSL-CM5A-LR under RCP8.5, project decreases in TAG and increases in precipitation, which implies warming will be distributed differently. In general, there is no clear dependency of the changes on RCP. This would not necessarily be expected as forcings/emissions are not always incrementally increased from one RCP to the next, particularly at the regional level.

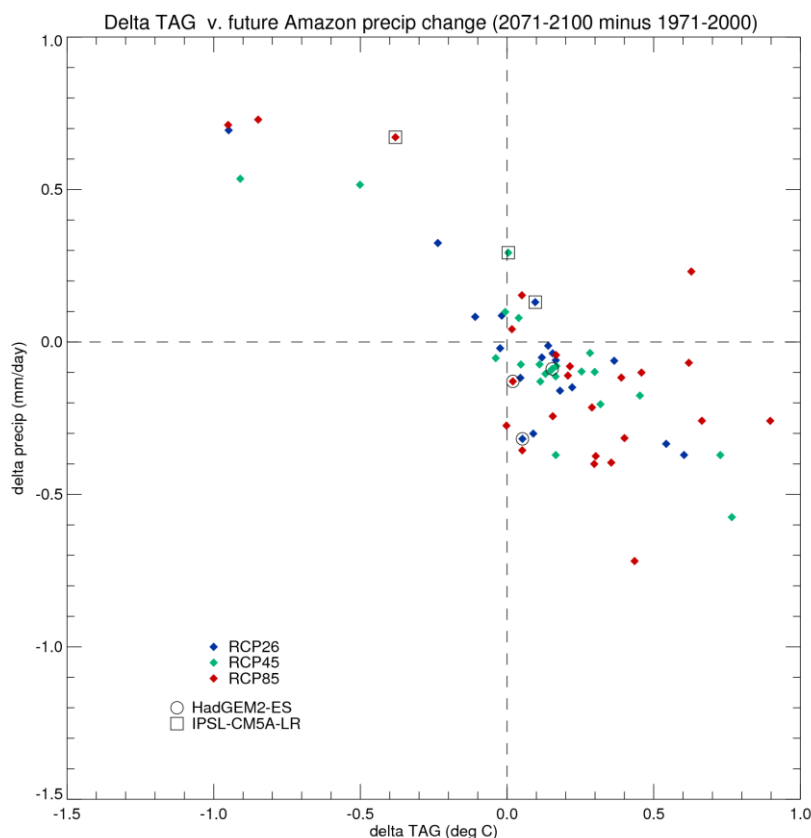


Figure 20. Change in JJA TAG versus change in Amazon basin precipitation (2061-2100 minus 1961-2000) in CMIP5 models and for RCPs 2.6, 4.5 and 8.5.

## 6. Role of CMIP5 Land Use: historical and future

As set out above, the RCPs include land cover change (LCC). The effects of LCC on both the past and future climate have recently been addressed in a multi-model approach in the context of the Land-Use and Climate, IDentification of robust impacts (LUCID) project (Pitman et al. 2009). The first LUCID set of simulations was carried out using seven GCMs to assess the biogeophysical effects of LCC between the preindustrial period and the present day.

The historical LCC, as simulated in LUCID models, had little climatic impact globally but produced important effects at the continental scale. For example, the LUCID models simulated a reduction in albedo over the historical period in response to the large deforestation in the northern extratropical lands. However, the models showed large spread in the magnitude of some effects of LCC (e.g. albedo), while other effects differ in both magnitude and sign (e.g. evapotranspiration). Such inter-model dispersion has two main causes, as discussed in Boisier et al. (2012): differences in the models' sensitivity to LCC and differences in land-cover maps prescribed in each of them. Although all the land surface models embedded in LUCID climate models used as reference the same crop and pasture extents for preindustrial and present day, modellers have implemented these using different procedures into their own standard vegetation maps. This has induced significant differences in the deforestation rates realised by each land surface model (ranging from ~ 4 to 10 million km<sup>2</sup> globally) and, therefore, in the simulated climate responses to LCC.

No specific future simulations were planned in CMIP5 to isolate the effects of LCC. To address this matter, a set of complementary simulations was designed in the context of LUCID (please see <http://www.mpimet.mpg.de/en/science/the-land-in-the-earth->

system/climate-biogeosphere-interaction/lucid-cmip5.html). In these, land use is fixed at 2005 levels, while the other drivers of change vary according to the RCP.

Brovkin et al. (2013 *in revision*) describe the projected climatic effects of LCC to the end of 21<sup>st</sup> century simulated in six fully coupled climate models (ESMs) under the RCP2.6 and RCP8.5 scenarios. Model results show small changes in near surface temperature and in other quantities, constrained to the regions that have experienced substantial land conversion (larger than 10%), and do not show significant climatic impacts on the global scale. Most models show reductions in land carbon storage due to LCC. Brovkin et al. suggest that the limited effects of LCC on the projected climate result from relatively weak land perturbations (if compared to the historical LCC). They also note that the future changes mainly concern low latitudes, where the differences in biophysical properties of the various land cover types are smaller than those of the temperate and boreal regions.

### **Projected land-use changes in the Amazon: RCPs and other scenarios**

Through land-use changes humans have significantly disturbed the Amazon forest during the last decades. The current deforestation rates in the Amazon will likely continue in the near future driven, within other factors, by the biofuel demand (Nepstad et al. 2008). Projected LCC during the 21<sup>st</sup> century within the Amazon basin based on the LUH (RCPs) dataset is very small, so the simulated climatic impact of LCC is also insignificant in the region, as the LUCID-CMIP5 set of simulations show (Brovkin et al. 2013 *in revision*).

Simulations following the LUCID protocol were also carried out at the Met Office with HadGEM2-ES, with an additional simulation to isolate the effect of LCC in RCP4.5 in addition to the LUCID standard 2.6 and 8.5. Consistent with the results found elsewhere in LUCID, the HadGEM2-ES simulated impact of RCP land use on the climate of Amazonia (Figure 21) in the 21<sup>st</sup> century appears to be negligible.

Brazil's National Space Research Institute (INPE) through the project PRODES estimates a total forest cover loss of around 35 million ha between 1990 and 2010 in the Brazilian Legal Amazon region. This recent trend is consistent with other estimates, such as that of the UN-FAO Forest Resources Assessments (FRA 2010) that reports a total deforestation from 1990 to 2010 of 55 and 70 million ha for the Brazilian Amazon and the whole Amazon basin, respectively. During the same period, the prescribed deforestation in the IPSL model based on LUH dataset reaches 16 million km<sup>2</sup> for the whole basin and taking the strongest scenario in terms of deforestation (RCP 2.6) for the 2006-2010 time-slice, i.e. more than four times lower than FAO estimates.

An overview of different historical and future scenarios of Amazonian deforestation is illustrated in Figure 22. The weak values resulting from LUH is manifest during the historical period (since 1950) when compared to the observations-based data. It is also clear that the resulting forest cover loss projected to the future based on the RCP scenarios are also extremely optimistic if compared with both the mitigation and non-policy scenarios proposed within the SimAmazonia framework (Soares-Filho et al. 2006). SimAmazonia takes into account recent observation-based forest clearing statistics (from PRODES), local socio-economical factors, governance conservation strategies and biophysical parameterizations to derive scenarios of land-use and forest cover.

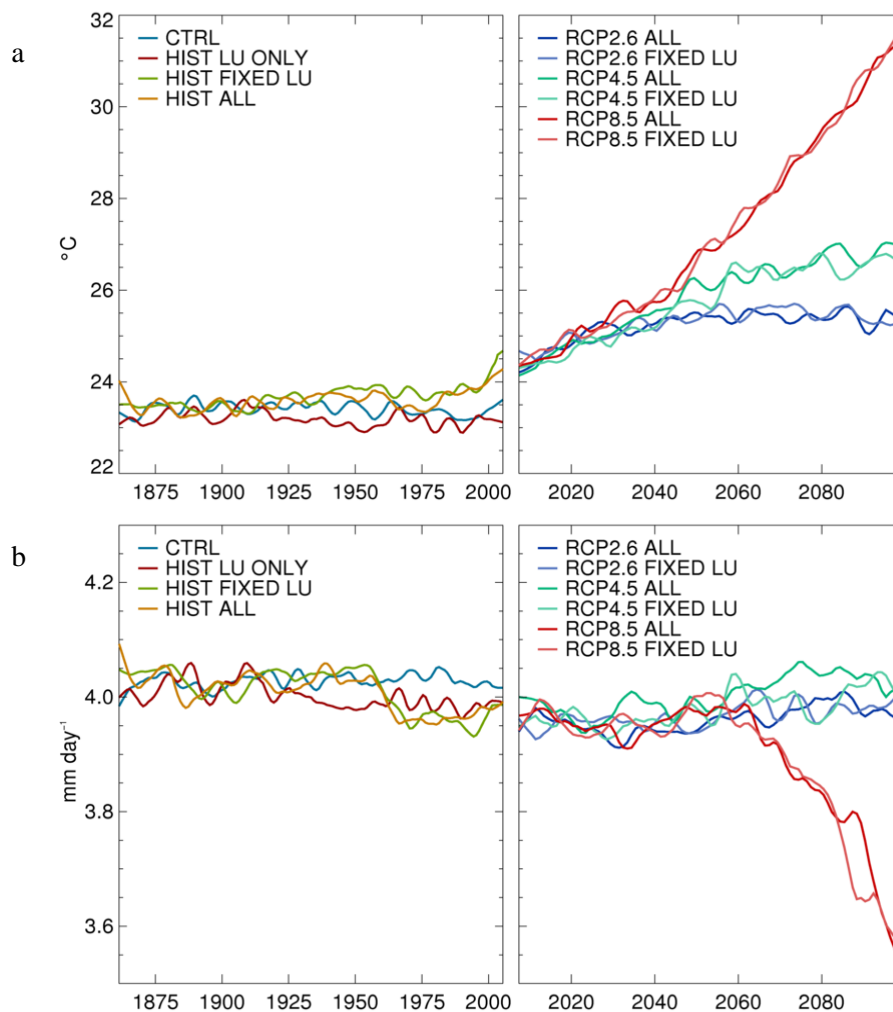


Figure 21. Temperature (a) and evapotranspiration (b) in the Amazon Basin simulated by HadGEM2-ES under historical forcings (left panel) and RCPs 2.6, 4.5 and 8.5 (right panel) with different combinations of climate and land use (LU) drivers. In the left panel, historical simulations were driven by: historical land use only, with no change in greenhouse gas concentrations (“HIST LU ONLY”: red line); greenhouse gas changes but with land use fixed at the initial state in 1860 (“HIST FIXED LU”: green line); and a combination of the previous two (“HIST ALL”: orange line). The control simulation with no external forcing is also shown (“CTRL”: blue line). In the right panel, dark lines (“ALL”) show simulations driven by greenhouse gas and land use changes for RCP2.6, RCP4.6 and RCP8.5, and faded lines (“FIXED LU”) show simulations driven with greenhouse gas changes but with land use fixed at the 2005 state.

The discrepancy between the LUH-based changes in land cover and the observation-based estimates during the historical period could in part result from the method adopted to include the agricultural data into LSMs (de Noblet-Ducoudre et al. 2012). However, the strength of such differences also denotes that the historical agricultural information provided by HYDE (the one used in LUH), although probably the most up-to-date and adequate dataset to be used in global-scale and long-term LCC studies, lacks realism at the regional scale. This is logical given the number of local factors behind the land-use evolution other than the changes in population density, principal driver used in the HYDE dataset (Goldewijk et al. 2011). Further, the LCC trajectories proposed in the CMIP5 framework (RCPs) do not appear either as realistic scenarios for regional-scale studies since they do not take into account recent observed LCC and do not well represent local (country-scale) complexities in the land-use

dynamics and their responses to global requirements. Land use effects on the Amazon climate need to be addressed with regional-scale scenarios such as SimAmazonia. Under AMAZALERT, new scenarios of land-use are being developed in order to address this requirement.

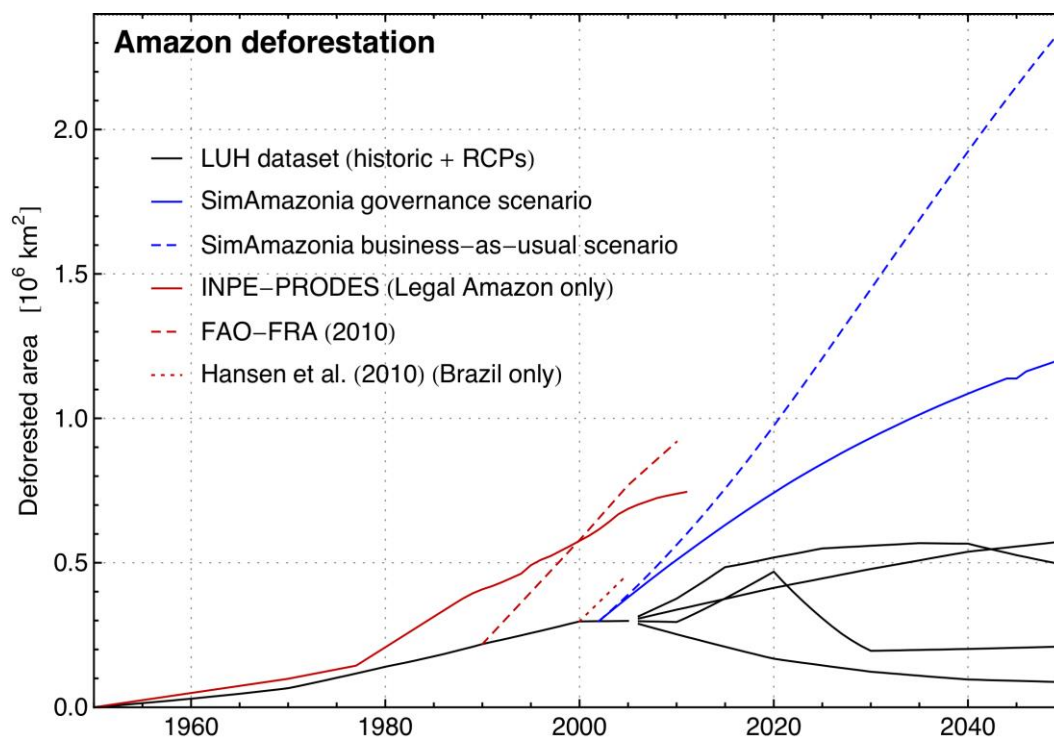


Figure 22. Total area deforested within the Amazon basin prescribed in ORCHIDEE based on LUH (black lines indicate the historical data and the four RCP scenarios) and based on SimAmazonia (blue; solid and dashed line indicate the governance and non-policy scenarios). Solid, dashed and dotted red lines indicate estimations of forest cover loss from different sources: PRODES (Brazilian Legal Amazon region only), FAO Global Forest Resources Assessment (2010) and Hansen et al. (2008; Brazil only). For clarity of display, the SimAmazonia and the observation-based deforestation time-series are shifted so that the first year of each matches the LUH curve.

## 7. Summary

This Deliverable has reported on the new CMIP5 projections of climate change in the Amazon basin. The centennial simulations have been carried out according to different scenarios of GHG concentrations, and include land use change consistent with development pathway and policy decisions. Thus, the implications of GHG and land-use on the changes in Amazonia can be explored in the CMIP5 multi-model ensemble. It presents an update to the CMIP3 projections of change that were reported in the IPCC AR4 (2007).

The CMIP5 ensemble comprises a significantly larger group of models than CMIP3, and the individual models are generally more complex. These models simulate reasonably well some aspects of the current climate of Amazonia and the wider region, such as the timing of the transitions in the seasonal cycle, and the mean temperatures in the region. Many of the models capture some characteristics of the important observed relationships between rainfall and SST anomalies including being able to simulate the correct sign of the relationships between wet season rainfall and the tropical Pacific and dry season rainfall and the tropical Atlantic.

However, as a whole, the ensemble simulates conditions that are too dry in the Amazon basin throughout the year, and in many models substantially so. This poses a challenge for interpreting changes in indicators of drought or other climate measures related to forest health, particularly where absolute values are thought to be important. It also has implications for the use of model output to drive offline impacts models.

The broad patterns of climate change projected by the CMIP5 ensemble are similar to those of CMIP3, and show that impacts increase under higher concentration scenarios. Temperature is projected to increase over South America, with regional maximum warming occurring over Amazonia. Increasing temperature, considered in isolation from other changes, has a detrimental effect on vegetation in Amazonia (Huntingford et al. 2013 *accepted*). Therefore, temperature must always be considered a potentially important stressor on the forest. The changes in rainfall projected by the ensemble are mixed over the Amazon basin, and vary by season. However, there is generally more agreement on drying in the eastern basin, particularly in the June to November period, with wetter conditions projected by the majority of models in the western basin, particularly in December to May. However, there is a spread in the model projections that spans zero, and over the Amazon basin itself, there is no clear scenario dependency apart from an increase in spread in RCP8.5 over 4.5 and 2.6.

Most models projections suggest the correlation between Amazon basin precipitation and tropical Pacific SSTs in DJF will remain unchanged. In the tropical Atlantic there is little consensus on the evolution of precipitation/SST correlations in JJA, and hence it may be practical to consider only the effect of SST changes rather than changes in the precipitation/SST relationship. In most models, projections are for increased warming in the northern relative to the southern tropical Atlantic corresponding to a reduction in dry season precipitation.

Experiments complementary to the CMIP5 centennial RCP simulations were carried out in order to isolate the impacts of land use change from the other drivers of change. Land use change in Amazonia over the 21<sup>st</sup> century is small, and does not have a discernable effect on climate. A comparison between observation-based estimates of historical deforestation rates and those in the RCP with largest change (RCP2.6) reveals that the RCP rates are substantially lower. Furthermore, they are optimistic in comparison with some previously developed bottom-up scenarios. It is suggested the historical land cover is not sufficiently accurate at the regional scale and also that RCP land use scenarios are unlikely to realistically represent changes at regional scales. Hence these data are in for investigating impacts of land use change in Amazonia in the future, and would benefit from improved region-specific scenarios. The new scenarios of land use change being developed by INPE through AMAZALERT will help to address this requirement.

## References

Aceituno, P., 1988: On the functioning of the Southern Oscillation in the South American Sector. Part I: Surface Climate. *Mon Weather Rev*, **116**, 505-524.

Aumont, O., and L. Bopp, 2006: Globalizing results from ocean in situ iron fertilization studies. *Global Biogeochem. Cycles*, **20**, GB2017.

Ball, J., T. Woodrow, and J. Berry, 1987: A model predicting stomatal conductance and its contribution to the control of photosynthesis under different environmental conditions. *Progress in Photosynthesis*, **4**, 221-224.

Betts, R. A., P. M. Cox, M. Collins, P. P. Harris, C. Huntingford, and C. D. Jones, 2004: The role of ecosystem-atmosphere interactions in simulated Amazonian precipitation decrease and forest dieback under global climate warming. *Theor. Appl. Climatol.*, **78**, 157-175.

Betts, R. A., and Coauthors, 2007: Projected increase in continental runoff due to plant responses to increasing carbon dioxide. *Nature*, **448**, 1037-U1035.

Betts, R. A., and Coauthors, 2013 *submitted*: Climate and land use change impacts on global terrestrial ecosystems, fire, and river flows in the HadGEM2-ES Earth System Model using the Representative Concentration Pathways. *Biogeosciences*.

Boisier, J. P., and Coauthors, 2012: Attributing the impacts of land-cover changes in temperate regions on surface temperature and heat fluxes to specific causes: Results from the first LUCID set of simulations. *J. Geophys. Res.-Atmos.*, **117**.

Brovkin, V., and Coauthors, 2013 *in revision*: Effect of anthropogenic land-use and land cover changes on climate and land carbon storage in CMIP5 projections for the 21st century. *J. Climate*.

Butt, N., P. A. de Oliveira, and M. H. Costa. 2011: Evidence that deforestation affects the onset of the rainy season in Rondonia, Brazil. *J. Geophys. Res.*, **116**, D11120, doi:10.1029/2010JD015174

Clark, D. B., and N. Gedney, 2008: Representing the effects of subgrid variability of soil moisture on runoff generation in a land surface model. *J. Geophys. Res.-Atmos.*, **113**.

Coe, M. T., M. H. Costa, and B. S. Soares-Filho, 2009: The influence of historical and potential future deforestation on the stream flow of the Amazon River – Land surface processes and atmospheric feedbacks. *J. Hydrol.*, **369**, 1-2, 165-174.

Collatz, G., M. Ribas-Carbo, and J. Berry, 1992: Coupled photosynthesis stomatal conductance model for leaves of C4 plants. *Aust J Plant Physiol*, **19**, 519-538.

Collins, M., and Coauthors, 2010: The impact of global warming on the tropical Pacific ocean and El Niño. *Nature Geosci.*, **3**, 391-397.

Collins, W. J., and Coauthors, 2011: Development and evaluation of an Earth-System model-HadGEM2. *Geosci Model Dev*, **4**, 1051-1075.

Costa, M. H. and J. A. Foley, 2000: Combined Effects of Deforestation and Doubled Atmospheric CO<sub>2</sub> Concentrations on the Climate of Amazonia. *J. Climate*, **13**, 1, 18-34.

Costa, M. H., A. Botta, and J. A. Cardille, 2003: Effects of large-scale changes in land cover on the discharge of the Tocantins River, Southeastern Amazonia. *J. Hydrol.*, **283**, 206-217.

Costa, M. H., S. N. M. Yanagi, P. J. O. P. Souza, A. Ribeiro, and E. J. P. Rocha, 2007: Climate change in Amazonia caused by soybean cropland expansion, as compared to caused by pastureland expansion. *Geophys. Res. Lett.*, **34**, L07706.

Cox, P. M., R. A. Betts, C. D. Jones, S. A. Spall, and I. J. Totterdell, 2000: Acceleration of global warming due to carbon-cycle feedbacks in a coupled climate model. *Nature*, **408**, 184-187.

Cox, P. M., 2001: Description of the 'TRIFFID' dynamic global vegetation model, [www.met-office.gov.uk/research/hadleycentre/pubs/HCTN/HCTN\\_24.pdf](http://www.met-office.gov.uk/research/hadleycentre/pubs/HCTN/HCTN_24.pdf) pp.

Cox, P. M., R. A. Betts, M. Collins, P. P. Harris, C. Huntingford, and C. D. Jones, 2004: Amazonian forest dieback under climate-carbon cycle projections for the 21st century. *Theor. Appl. Climatol.*, **78**, 137-156.

Cox, P. M., and Coauthors, 2008: Increasing risk of Amazonian drought due to decreasing aerosol pollution. *Nature*, **453**, 212-217.

Cox, P. M., D. Pearson, B. B. Booth, P. Friedlingstein, C. Huntingford, C. D. Jones, and C. M. Luke, 2013: Sensitivity of tropical carbon to climate change constrained by carbon dioxide variability. *Nature*, **494**, 341-344.

Davie, J. C. S., and Coauthors, 2013 *in open review*: Comparing projections of future changes in runoff and water resources from hydrological and ecosystem models in ISI-MIP. *Earth System Dynamics Discussion*, **4**, 279–315.

de Noblet-Ducoudre, N., and Coauthors, 2012: Determining Robust Impacts of Land-Use-Induced Land Cover Changes on Surface Climate over North America and Eurasia: Results from the First Set of LUCID Experiments. *J. Climate*, **25**, 3261-3281.

Ducoudré, N., K. Laval, and A. Perrier, 1993: SECHIBA, a new set of parameterizations of the hydrologic exchanges at the land-atmosphere interface within the LMD Atmospheric General Circulation Model. *J. Climate*, **6**, 248-273.

Dufresne, J.-L. e. a., 2013 *accepted*: Climate change projections using the IPSL-CM5 Earth System Model: from CMIP3 to CMIP5. *Clim. Dynam.*

Espinoza, J. C., and Coauthors, 2011: Climate variability and extreme drought in the upper Solimoes River (western Amazon Basin): Understanding the exceptional 2010 drought. *Geophys. Res. Lett.*, **38**.

FAO, 2010: Global Forest Resources Assessment 2010.

Farquhar, G., S. von Caemmerer, and J. Berry, 1980: A biochemical model of photosynthesis CO<sub>2</sub> fixation in leaves of C<sub>3</sub> species. *Planta*, **149**, 78-90.

FRA, 2010: Global Forest Resources Assessment 2010.

Gedney, N., P. M. Cox, and C. Huntingford, 2004: Climate feedback from wetland methane emissions. *Geophys. Res. Lett.*, **31**.

Goldewijk, K. K., A. Beusen, G. van Drecht, and M. de Vos, 2011: The HYDE 3.1 spatially explicit database of human-induced global land-use change over the past 12,000 years. *Global Ecol. Biogeogr.*, **20**, 73-86.

Golding, N., and R. Betts, 2008: Fire risk in Amazonia due to climate change in the HadCM3 climate model: Potential interactions with deforestation. *Global Biogeochem. Cycles*, **22**, Gb4007.

Good, P., J. A. Lowe, M. Collins, and W. Moufouma-Okia, 2008: An objective tropical Atlantic sea surface temperature gradient index for studies of south Amazon dry-season climate variability and change. *Phil. Trans. R. Soc. B.*, **363**, 1761-1766.

Good, P., C. Jones, J. Lowe, R. Betts, and N. Gedney, 2013: Comparing Tropical Forest Projections from Two Generations of Hadley Centre Earth System Models, HadGEM2-ES and HadCM3LC. *J. Climate*, **26**, 495-511.

Hansen, M. C., Y. E. Shimabukuro, P. Potapov, and K. Pittman, 2008: Comparing annual MODIS and PRODES forest cover change data for advancing monitoring of Brazilian forest cover. *Remote Sens. Environ.*, **112**, 3784-3793.

Harris, P. P., C. Huntingford, and P. M. Cox, 2008: Amazon Basin climate under global warming: the role of the sea surface temperature. *Phil. Trans. R. Soc. B.*, **363**, 1753-1759.

Hourdin, F., and Coauthors, 2012: LMDZ5B: the atmospheric component of the IPSL climate model with revisited parameterizations for clouds and convection. *Clim. Dynam.*, 1-30.

Huntingford, C., and Coauthors, 2013 *accepted*: Simulated resilience of tropical rainforests to CO<sub>2</sub>-induced climate change. *Nature Geosci.*

Hurtt, G. C., and Coauthors, 2011: Harmonization of land-use scenarios for the period 1500-2100: 600 years of global gridded annual land-use transitions, wood harvest, and resulting secondary lands. *Climatic Change*, **109**, 117-161.

Intergovernmental Panel on Climate Change IPCC, 2007: *Climate Change 2007: The Physical Science Basis. Contribution of Working Group I to the Fourth Assessment Report of the Intergovernmental Panel on Climate Change* Cambridge University Press, 996 pp.

Jones, C., J. Lowe, S. Liddicoat, and R. Betts, 2009: Committed terrestrial ecosystem changes due to climate change. *Nature Geosci.*, **2**, 484-487.

Krinner, G., and Coauthors, 2005: A dynamic global vegetation model for studies of the coupled atmosphere-biosphere system. *Global Biogeochem. Cycles*, **19**.

Liebmann, B., and J. A. Marengo, 2001: Interannual variability of the rainy season and rainfall in the Brazilian Amazon basin. *J. Climate*, **14**, 4308-4318.

Loveland, T. R., B. C. Reed, J. F. Brown, D. O. Ohlen, Z. Zhu, L. Yang, and J. W. Merchant, 2000: Development of a global land cover characteristics database and IGBP DISCover from 1 km AVHRR data. *Int J Remote Sens*, **21**, 1303-1330.

Madec, G., 2008: NEMO ocean engine. Technical note, IPSL. Available at [http://www.nemo121ocean.eu/content/download/15482/73217/file/NEMO\\_book\\_v3\\_3.pdf](http://www.nemo121ocean.eu/content/download/15482/73217/file/NEMO_book_v3_3.pdf).

Malhado, A. C. M, G. F. Pires, and M H. Costa, 2010: Cerrado conservation is essential to protect the Amazon rainforest. *Ambio*, **39**, 580-584. PMID:21141777. <http://dx.doi.org/10.1007/s13280-010-0084-6>

Malhi, Y., and Coauthors, 2009: Exploring the likelihood and mechanism of a climate-change-induced dieback of the Amazon rainforest. *Proc. Natl. Acad. Sci. USA*, **106**, 20610-20615.

Marengo, J. A., 1992: Interannual variability of surface climate in the Amazon Basin. *Int. J. Climatol.*, **12** 853-863.

Marengo, J. A., 2004: Interdecadal variability and trends of rainfall across the Amazon basin. *Theor. Appl. Climatol.*, **78**, 79-96.

Marengo, J. A., and Coauthors, 2008: The drought of Amazonia in 2005. *J. Climate*, **21**, 495-516.

Marengo, J. A., and Coauthors, 2011a: Dangerous Climate Change in Brazil: A Brazil-UK analysis of climate change and deforestation impacts in the Amazon.

Marengo, J. A., J. Tomasella, L. M. Alves, W. R. Soares, and D. A. Rodriguez, 2011b: The drought of 2010 in the context of historical droughts in the Amazon region. *Geophys. Res. Lett.*, **38**.

Martin, G. M., and Coauthors, 2011: The HadGEM2 family of Met Office Unified Model climate configurations. *Geosci Model Dev*, **4**, 723-757.

Mercado, L. M., N. Bellouin, S. Sitch, O. Boucher, C. Huntingford, M. Wild, and P. M. Cox, 2009: Impact of changes in diffuse radiation on the global land carbon sink. *Nature*, **458**, 1014-U1087.

Moss, R. H., and Coauthors, 2010: The next generation of scenarios for climate change research and assessment. *Nature*, **463**, 747-756.

Nakićenović, N., and Coauthors, 2000: *Special Report on Emissions Scenarios*. Intergovernmental Panel on Climate Change. Cambridge University Press.

Nepstad, D. C., and Coauthors, 1999: Large-scale impoverishment of Amazonian forests by logging and fire. *Nature*, **398**, 6727, 505-508.

Nepstad, D. C., C. M. Stickler, B. Soares, and F. Merry, 2008: Interactions among Amazon land use, forests and climate: prospects for a near-term forest tipping point. *Phil. Trans. R. Soc. B.*, **363**, 1737-1746.

Nobre, C. A., P. Sellers, and J. Shukla, 1991: Amazonian deforestation and regional climate change. *J. Climate*, **4**, 957-988.

Oki, T., and Y. C. Sud, 1998: Design of Total Runoff Integrating Pathways (TRIP)—A Global River Channel Network. *Earth Interact.*, **2**, 1-37.

Pitman, A. J., and Coauthors, 2009: Uncertainties in climate responses to past land cover change: First results from the LUCID intercomparison study. *Geophys. Res. Lett.*, **36**.

Rammig A., and Coauthors, 2010: Estimating the risk of Amazonian forest dieback. *New Phytologist*, **187**, 694-706.

Ronchail, J., G. Cochonneau, M. Molinier, J. L. Guyot, A. G. D. Chaves, V. Guimaraes, and E. de Oliveira, 2002: Interannual rainfall variability in the Amazon basin and sea-surface temperatures in the equatorial Pacific and the tropical Atlantic Oceans. *Int. J. Climatol.*, **22**, 1663-1686.

Ropelewski, C. F., and M. S. Halpert, 1987: Global and Regional Scale Precipitation Patterns Associated with the El-Niño Southern Oscillation. *Mon Weather Rev*, **115**, 1606-1626.

Ruimy, A., G. Dedieu, and B. Saugier, 1996: TURC: A diagnostic model of continental gross primary productivity and net primary productivity. *Global Biogeochem. Cycles*, **10**, 269-285.

Salazar, L. F., C. Nobre, and M. D. Oyama, 2007: Climate change consequences on the biome distribution in tropical South America. *Geophys. Res. Lett.*, **34**, L09708.

Salazar, L. F., and C. A. Nobre, 2010: Climate change and thresholds of biome shifts in Amazonia. *Geophys. Res. Lett.*, **37**, L17706.

Sampaio, G., and Coauthors, 2007: Regional climate change over eastern Amazonia caused by pasture and soybean cropland expansion. *Geophys. Res. Lett.*, **34**, L17709, doi:10.1029/2007GL030612

Scholze M., W. Knorr, N. W. Arnell, and I. C. Prentice, 2006: A climate-change risk analysis for world ecosystems. *Proc. Natl. Acad. Sci. USA*, **103**, 13116–13120.

Soares-Filho, B. S., and Coauthors, 2006: Modelling conservation in the Amazon basin. *Nature*, **440**, 520-523.

Taylor, K. E., R. J. Stouffer, and G. A. Meehl, 2012: An Overview of Cmp5 and the Experiment Design. *Bull. Am. Meteorol. Soc.*, **93**, 485-498.

van Vuuren, D. P., and Coauthors, 2011: The representative concentration pathways: an overview. *Climatic Change*, **109**, 5-31.

Yeh, S. W., J. S. Kug, B. Dewitte, M. H. Kwon, B. P. Kirtman, and F. F. Jin, 2009: El Niño in a changing climate. *Nature*, **461**, 511-U570.

Yeh, S. W., Y. G. Ham, and J. Y. Lee, 2012: Changes in the Tropical Pacific SST Trend from CMIP3 to CMIP5 and Its Implication of ENSO. *J. Climate*, **25**, 7764-7771.

Yoon, J. H., and N. Zeng, 2010: An Atlantic influence on Amazon rainfall. *Clim. Dynam.*, **34**, 249-264.

## Publications

Papers: Published, in review, in preparation

1. Seiler, C., R. W. A. Hutjes, and P. Kabat, 2013: Climate variability and trends in Bolivia. *J. Appl. Meteorol. and Climatol*, **52**, 130-146.
2. Seiler, C., R. W. A. Hutjes, and P. Kabat, 2013 *in review*: Likely ranges of climate change in Bolivia.
3. Joetzer, E., H. Douville, C. Delire, P. Ciais, 2013 *in prep.*: Present-day and future Amazonian precipitation in global climate models: CMIP5 versus CMIP3
4. Alves, L., et al., 2013 *in prep.*: Evaluation of the South American climate in IPCC AR5 climate model simulations of the twentieth century.